MOLECULAR AND CELLULAR BIOLOGY, Dec. 1997, p. 6953–6969 Vol. 17, No. 12
0270-7306/97/$04.00+0

Sin Mutations of Histone H3: Influence on Nucleosome Core Structure and Function

HITOSHI KURUMIZAKA AND ALAN P. WOLFFE*

Laboratory of Molecular Embryology, National Institute of Child Health and Human Development, Bethesda, Maryland 20892-5431

Received 17 July 1997/Returned for modification 3 September 1997/Accepted 5 September 1997

Sin mutations in *Saccharomyces cerevisiae* alleviate transcriptional defects that result from the inactivation of the yeast SWI/SNF complex. We have investigated the structural and functional consequences for the nucleosome of Sin mutations in histone H3. We directly test the hypothesis that mutations in histone H3 leading to a SWI/SNF-independent (Sin) phenotype in yeast lead to nucleosomal destabilization. In certain instances this is shown to be true; however, nucleosomal destabilization does not always occur. Topoisomerase I-mediated relaxation of minichromosomes assembled with either mutant histone H3 or wild-type H3 together with histones H2A, H2B, and H4 indicates that DNA is constrained into nucleosomal structures containing either mutant or wild-type proteins. However, nucleosomes containing particular mutant H3 molecules (R116-H and T118-I) are more accessible to digestion by micrococcal nuclease and do not constrain DNA in a precise rotational position, as revealed by digestion with DNase I. This result establishes that Sin mutations in histone H3 located close to the dyad axis can destabilize histone-DNA contacts at the periphery of the nucleosome core. Other nucleosomes containing a distinct mutant H3 molecule (E105-K) associated with a Sin phenotype show very little change in nucleosome structure and stability compared to wild-type nucleosomes. Both mutant and wild-type nucleosomes continue to restrict the binding of either TATA-binding protein/transcription factor IIA (TFIIA) or the RNA polymerase III transcription machinery. Thus, different Sin mutations in histone H3 alter the stability of histone-DNA interactions to various extents in the nucleosome while maintaining the fundamental architecture of the nucleosome and contributing to a common Sin phenotype.

A substantial component of transcriptional regulation depends on the interplay between transcription factors and histones at specific sites within the enhancers and promoters of eukaryotic genes (9, 10, 82). In the yeast *Saccharomyces cerevisiae*, the outcome of this interaction can be influenced by the products of the several genes originally identified by defects in mating type switching (SWI) and/or sucrose fermentation (SNF [sucrose nonfermenter]) (53, 67, 101). The SWI/SNF complex is a multicomponent molecular machine required for the transcriptional induction of many, but not all, genes and for the functions of several heterologous activators in yeast (14, 17, 68, 69). Genetic and biochemical studies of the yeast proteins and their larger eukaryotic homologs suggest that one function of the SWI/SNF complex is to help transcription factors overcome the repressive effects of nucleosome assembly on transcription (20, 42, 48–50).

Powerful genetic and physical mapping evidence has established a role for nucleosomes as transcriptional repressors in yeast (1, 2, 33, 81). Alterations in histone abundance (34, 35), histone stoichiometry (19, 26), and histone sequence (27, 44, 46, 49) can all relieve transcriptional repression for particular yeast genes. General alterations in chromatin structure that lead to specific changes in transcription might be explained by both the positioning of nucleosomes within specific regulatory structures (24, 76, 77) and the targeted recruitment of particular molecular machines and/or enzyme complexes that modify chromatin structure (12, 67, 101). Exactly how chromatin structure might be modified or disrupted by the targeted recruitment of molecular machines such as the SWI/SNF complex remains unknown. However, the SWI/SNF complex has the capacity to alter the rotational positioning of DNA on the surface of a nucleosome core and increases the accessibility of nucleosomal DNA to transcription factors in vitro (20, 50). The SWI/SNF complex also has the capacity to interact with DNA independent of any gene specific targeting (73).

An important clue to the role of the SWI/SNF complex in disrupting chromatin structure came from the isolation of Sin (switch-independent) mutations, which alleviate transcriptional defects due to the inactivation of the yeast SWI/SNF complex (48, 49, 66). Sin alleles can result from single point mutations in histone H3 or H4; however, the *SIN2* gene itself is identical to *HHT2*, which encodes histone H3 (49). Localization of the amino acid changes in histone H3 and H4 that lead to the Sin phenotype offers insight into the potential function of the SWI/SNF complex (41, 49, 102). Arents et al. have determined the structure of the histone octamer around which DNA is wrapped in the nucleosome (3, 4). Each core histone has (i) an amino-terminal tail domain that reaches outside the two superhelical turns of DNA within the nucleosome and (ii) a carboxy-terminal histone fold domain that is involved in histone-histone interactions inside nucleosomal DNA. The carboxy-terminal domains of each core histone are predominantly α-helical, with a long central helix bordered on each side by a loop segment and a shorter helix (Fig. 1A). Histone heterodimerization leads to the loop segments from each half of the dimer being paired to form eight parallel β-bridge segments, two of which are found in each of the heterodimers (H3 and H4) and (H2A and H2B). Each β-bridge segment is associated with at least two positively charged amino acids, which are available to make contact with DNA on the surface of the histone octamer (4). A second potential DNA binding surface arises from the pairing of the amino-terminal end of the first helical domain of each of the

* Corresponding author. Mailing address: Laboratory of Molecular Embryology, National Institute of Child Health and Human Development, NIH, Bldg. 18T, Rm. 106, Bethesda, MD 20892-5431. Phone: (301) 402-2722. Fax: (301) 402-1323. E-mail: awlme@helix.nih.gov.

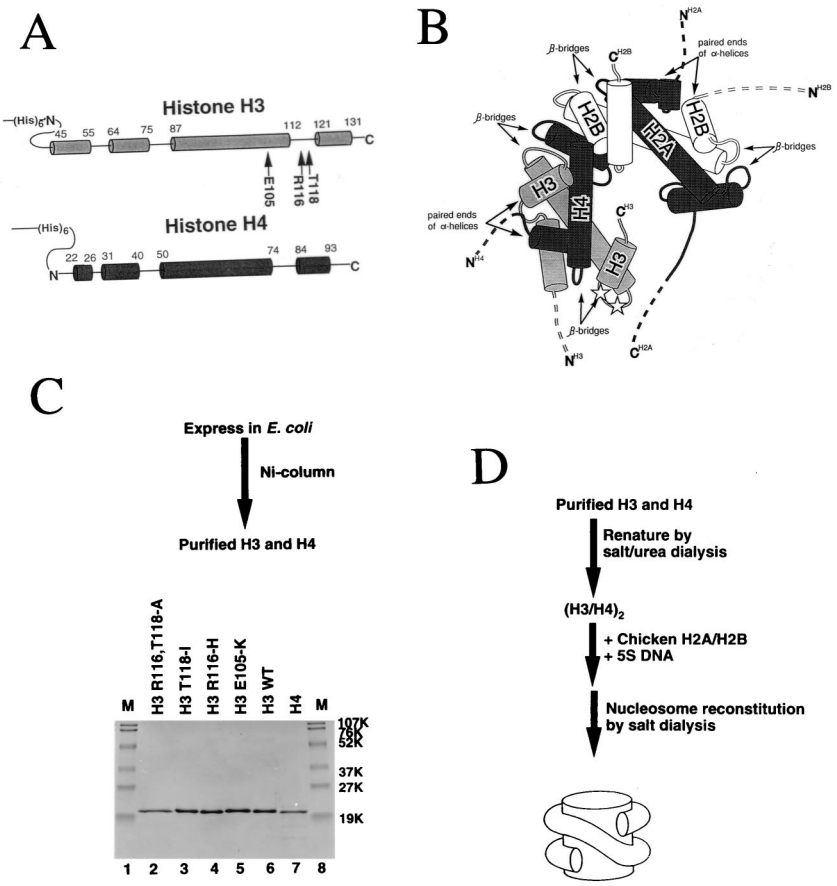

FIG. 1. Strategy for analyzing nucleosomes containing mutant histones in vitro. (A) Recombinant histones H3 and H4. α-Helices are indicated by cylinders. Residues which were mutated in histone H3 are indicated by arrows. (B) Locations of Sin mutations in histone H3 in H3-H4 dimer. Relative locations of H2A-H2B and H3-H4 dimers are presented. Stars indicate amino acid residues of Arg116 and Thr118 in histone H3 (3, 4). (C) Purified histones (1 μg) were analyzed by SDS–18% polyacrylamide gel electrophoresis. Lanes 2 to 5, mutant histones H3, R116,T118-A, T118-I, R116-H, and E105-K, respectively; lanes 6 and 7, recombinant wild-type (WT) histones H3 and H4, respectively; lanes 1 and 8, molecular weight markers (M). (D) Strategy for reconstituting nucleosomes by recombinant histones. Purified recombinant histones H3 and H4 were incubated in the presence of 6 M urea, and $(H3\text{-}H4)_2$ tetramers were reconstituted by salt-urea dialysis. Nucleosomes were reconstituted with chicken histones H2A and H2B and 5S DNA by salt dialysis (Materials and Methods).

histones in the heterodimers (Fig. 1B). The eight parallel β-bridges and four paired ends of helices provide 12 potential DNA contact sites that are regularly arranged along the ramp on which the double helix has been proposed to be wound (4). The mutations in histones H3 and H4 found in the Sin^- alleles cluster in one β-bridge motif within the H3-H4 heterodimer. Because of the juxtaposition of the two H3-H4 heterodimers at the dyad axis of the nucleosome (3), these mutations have the potential to disrupt histone-DNA interactions involving the central turn of DNA at the dyad axis. This could have a major impact on the integrity of both the nucleosome and higher-order chromatin structures and thereby relieve the requirement for the SWI/SNF complex to disrupt chromatin structure as a prerequisite for recruitment of other components of the transcriptional machinery.

In this work, we have examined the consequences of the Sin2 mutations of histone H3 for nucleosome assembly, structure, and stability in vitro. We find that although Sin2 mutations of H3 assemble nucleosomes and wrap DNA leading to the same topological constraints as wild-type histones, the nucleosomes containing certain mutant H3 proteins have altered accessibility to micrococcal nuclease (MNase) and DNase I. This finding establishes that Sin2 mutations can lead to a general alteration in histone-DNA contacts within the nucleosome. Other Sin2 mutations of H3 assemble nucleosomes comparable in stability to those containing wild-type H3. The alterations in nuclease cleavage observed with the Sin2 mutants that labilize the nucleosome core mirror the influence of the SWI/SNF complex on nucleosome cores in vitro (20, 50). Nevertheless, we find that nucleosomes containing mutant H3 constrain DNA in a comparable manner to wild-type nucleosomes with respect to both the binding of TATA-binding protein (TBP)/transcription factor IIA (TFIIA) and the RNA polymerase III transcriptional machinery. The implications of this result for SWI/SNF function are discussed.

MATERIALS AND METHODS

Plasmids and DNA fragments. The construction of plasmid pX5S 197-2, containing two tandem repeats of the 5S RNA gene, has been described elsewhere (87). This plasmid DNA molecule was used for chromatin reconstitution. For certain experiments, a 424-bp *Xba*I-*Xho*I fragment derived from plasmid pX5S 197-2 was isolated from nondenaturing acrylamide gels for nucleosome reconstitution after end labeling at the *Xba*I site with T7 polynucleotide kinase or Klenow fragment (New England Biolabs). This fragment was reconstituted into nucleosomes. A second DNA fragment used in these studies was a 238-bp *Hpa*II-*Dde*I fragment derived from plasmid pXbs-1 containing the *Xenopus borealis* somatic 5S RNA gene was radiolabeled on the coding strand at the *Hpa*II site 102 bp upstream from the initiation site for transcription of the 5S gene (+1) as described previously (71).

Sin2 mutations in histone H3; purification of recombinant tetramers of $(H3\text{-}H4)_2$. DNA fragments containing *Xenopus* histones H3 and H4 (65) were cloned into the *Nhe*I site and *Eco*RI site, respectively, of the pRSET plasmid vector (Invitrogen, San Diego, Calif.). Recombinant histones H3 and H4 were expressed in *Escherichia coli* as His-tagged proteins and purified by Ni column chromatography. The recombinant H3 contains the amino-terminal sequence Met-Arg-Gly-Ser-His-His-His-His-His-His-Gly-Met-Ala-Ser-Asp-Tyr-Lys-Asp-Asp-Asp-Asp-Lys, and recombinant H4 contains the amino-terminal sequence Met-Arg-Gly-Ser-His-His-His-His-His-His-Gly-Met-Ala-Ser-Met-Thr-Gly-Gly-Gln-Met-Gly-Arg-Asp-Leu-Tyr-Asp-Asp-Asp-Asp-Lys-Asp-Pro-Ser-Ser-Arg-Ser-Ala-Ala-Gly-Thr-Met-Glu-Ala-Ser-Asp-Tyr-Lys-Asp-Asp-Asp-Asp-Lys. The mutations in histone H3 were introduced by PCR (28). Recombinant histones H3 and H4 were expressed in *E. coli* as His-tagged proteins by T7 RNA polymerase. Cells which express recombinant histones were harvested and disrupted by sonication in buffer containing 20 mM Tris-HCl (pH 7.9), 0.5 M NaCl, and 10% glycerol. The cell suspension was centrifuged at 35,000 rpm for 1 h at 4°C to separate soluble and insoluble fractions. Recombinant histones were recovered in the insoluble fraction and dissolved in buffer containing 20 mM Tris-HCl (pH 7.9), 0.5 M NaCl, 5 mM imidazole, and 6 M urea. Then the protein solution containing recombinant histones was applied to an Ni column (ProBond; Invitrogen). Recombinant histones were eluted by a linear gradient of imidazole from 5 to 300 mM. Concentrations of purified recombinant histones were estimated by the modified Folin method (Pierce), and stoichiometric amounts of histones H3 and H4 were mixed in the presence of 2 M NaCl and 6 M urea. $(H3\text{-}H4)_2$ tetramers were reconstituted by decreasing of concentration of urea until 0 M by dialysis. The concentrations of wild-type $(H3\text{-}H4)_2$ and mutant $(H3\text{-}H4)_2$ tetramers were determined by the use of Coomassie blue G-250 (Bio-Rad protein assay kit).

Nucleosome reconstitution. For the salt dialysis method using purified histones (78), radiolabeled DNA (500 ng) and unlabeled DNA (4.5 μg) were mixed with histone octamers in 2.0 M NaCl. The final DNA concentration was 0.1 mg/ml, and the histone octamer concentration was 1.0 mol of octamer/mol of DNA repeat. Samples were then dialyzed at 4°C against 10 mM Tris-HCl (pH 7.5)–1 mM EDTA–0.1 mM phenylmethylsulfonyl fluoride (PMSF)–1 mM 2-mercaptoethanol and NaCl as follows: 2.0 M NaCl, 1 h; 1.5 M NaCl, 4 h; 1 M NaCl, 4 h; and 0.75 M NaCl, 4 h. The final dialysis was overnight into 10 mM Tris-HCl (pH 7.5)–1 mM EDTA–1 mM 2-mercaptoethanol at 4°C. The products contained naked DNA and mono-, di-, and trinucleosome cores.

After reconstitution, the oligonucleosome cores were loaded on 5 to 20% sucrose gradients containing 10 mM Tris-HCl (pH 7.5) 1 mM EDTA, and 0.1 mM PMSF and then centrifuged for 16 h at 35,000 rpm at 4°C in a Beckman SW41 rotor. Fractions were collected and analyzed in nucleoprotein agarose (0.7%) gels in 0.5× TBE (1× TBE is 90 mM Tris base, 90 mM boric acid, and 2.5 mM EDTA). Fractions containing mono-, di-, or trinucleosomes were pooled separately, concentrated to ~2.5μg/ml in a Microcon-30 (Amicon), and dialyzed against 10 mM Tris-HCl (pH 7.5)–0.1 mM EDTA–1 mM 2-mercaptoethanol overnight at 4°C. Samples were stored on ice until use. We always checked for the presence of spontaneous dissociation on nucleosomes by polyacrylamide gel electrophoresis (31). Chicken erythrocyte oligonucleosomes (chromatin lengths of 1 to 30 nucleosomes) were prepared, after removal of linker histones (55), and used as a control for isolation of the native dinucleosome complex.

To determine histone stoichiometry in reconstituted nucleosomes, we scaled up our preparations. Plasmid DNA pX5S 197-2 (10.5 μg) or the 424-bp DNA fragment from this plasmid (5 μg) was incubated with masses of core histones sufficient to allow one histone per 180 bp in buffer containing 10 mM Tris (pH 8.0), 1 mM EDTA, 1 mM 2-mercaptoethanol, and 2 M NaCl. Nucleosomes were reconstituted by the salt dialysis method (as described above). Nucleosomes reconstituted on plasmid DNA were separated by 0.7% agarose gel electrophoresis in buffer containing 45 mM Tris, 45 mM boric acid, and 1 mM EDTA and then electroeluted. Histones incorporated into nucleosomes were precipitated with 20% trichloroacetic acid and washed twice with 200 μl of acetone. Proteins were analyzed by sodium dodecyl sulfate (SDS)–18% polyacrylamide gel electrophoresis and stained with silver (107). Nucleosomes reconstituted on the 424-bp DNA fragment were fractionated by 5 to 20% sucrose gradients as described above and precipitated with 20% trichloroacetic acid. Proteins were analyzed by SDS–18% polyacrylamide gel electrophoresis and stained with silver (107).

Topological assay. Core histones (4, 8, and 12 μg) were incubated with 5 μg of plasmid DNA (pX5S 197-2, 3,624 bp) in the presence of 2.0 M NaCl. The concentration of NaCl was decreased gradually (2.0, 1.5, 1.2, 1.0, 0.8, 0.6, and 0 M) to reconstitute nucleosomes by the salt dialysis method. Reconstituted nucleosomes (ca. 200 ng) were analyzed on a 1% agarose gel. To assess nucleosome assembly, reconstituted nucleosomes were treated with 2.4 U of eukaryotic topoisomerase I (Gibco BRL) at 37°C for 30 min. Reactions were terminated by the addition of 1.5% SDS, and the plasmid DNAs were extracted with phenol-chloroform. DNA topoisomers were separated 1% agarose gel electrophoresis and were visualized by ethidium bromide staining. To determine the number of superhelical turns, marker DNA containing a defined number of negative superhelical turns was prepared (18) and resolved together with DNA isolated from minichromosomes on 1% agarose gels containing chloroquine (90 μg/ml) (18).

DNase I and hydroxyl radical footprinting. Reconstituted nucleosomes were treated with either DNase I or hydroxyl radicals before nucleoprotein complexes were resolved on preparative 0.7% agarose gels (104). Samples contained labeled dinucleosomes (60 ng of DNA) and chicken erythrocyte core particles (~1 μg). Mg^{2+} was adjusted to 4 mM concomitantly with addition of DNase I. Naked DNA was digested with 12 ng of DNase I (Gibco BRL); nucleosome cores were digested with 30 to 60 ng of enzyme. DNase I reactions were carried out at room temperature for 1 min and terminated by the addition of EDTA (5 mM). Glycerol (5%, vol/vol) was added to the sample, and the entire reaction volume was loaded on a preparative gel. The hydroxyl radical reaction was carried out as described previously (38). Free radical reactions were quenched with the addition of glycerol to a concentration of 5%, and the entire volume was applied to a gel as described above. After electrophoresis, bound or nucleosome complexes were excised from the gel. DNA from these complexes was isolated and analyzed by denaturing polyacrylamide (6%) gel electrophoresis. Specific DNA markers were produced by Maxam and Gilbert cleavage at G residues.

MNase mapping. Nucleosomes were reconstituted on plasmid or on linear DNA fragments (424 or 238 bp as indicated) by the salt dialysis method (see above). Reconstituted chromatin (200 ng of DNA) was digested with 0.075 to 2 U of MNase (Worthington Biochemical Company) for 5 min at 22°C. Ca^{2+} was adjusted to 0.5 mM concomitantly with addition of MNase. Digestions were terminated with addition of EDTA (5 mM), SDS (0.25%, wt/vol), and proteinase K (1 mg/ml; Gibco BRL). The DNA was recovered and 5′-end labeled with [γ-^{32}P]ATP and T4 polynucleotide kinase, and the end-labeled DNA fragments were separated by electrophoresis in nondenaturing 6% polyacrylamide gels.

Nucleosome mobility experiments. One- and two-dimensional gel experiments to show the distribution and redistribution, respectively, of nucleosome cores were performed following established procedures (58), with slight modifications. Reconstituted nucleosomes were loaded onto nondenaturing 4% polyacrylamide (29:1 acrylamide/bisacrylamide) gels at 4°C in 0.5× TBE. The gels were run at a maximum of 10 V/cm. For the one-dimensional gel, the gel was dried and exposed for autoradiography. For the two-dimensional gels, each lane was cut in half lengthwise. One half of each lane was left at 4°C, and the other was sealed and immersed at 37°C for 1 h. The gel strips were then arranged on top of a second nondenaturing gel in the cold, and the second dimension was electrophoresed at 4°C under the same conditions as the first dimension.

Transcription reactions for dinucleosomes. Nucleosomal complexes separated by sucrose gradient centrifugation from free histones and naked DNA were used as templates for transcription in an extract from *Xenopus* oocyte nuclei. Oocyte nuclear extract was prepared as described previously (11). Transcription reaction conditions were as follows. Radiolabeled template (10 ng) was added to 10 μl of reaction mixture containing 5 μl of nuclear extract in J buffer (10 mM HEPES [pH 7.4], 50 mM KCl, 7 mM $MgCl_2$, 2.5 mM dithiothreitol, RNasin [0.25 U/μl; Gibco BRL], 0.1 mM EDTA) and preincubated for 20 min before addition of exogenous triphosphates (250 μM ATP, CTP, and GTP plus 50 μM UTP) and 2.5μCi of [α-^{32}P]UTP. The reaction temperature was 22°C. Labeling was continued for 40 min after preincubation. Radiolabeled transcripts were extracted with phenol, precipitated with ethanol, and analyzed by electrophoresis in a 6% denaturing polyacrylamide gel. The level of 5S RNA transcription was quantitated with a Molecular Dynamics PhosphorImager. The radiolabeled 5S DNA template served as an internal control for recovery.

TBP/TFIIA binding studies. The two subunits of TFIIA were expressed in *E. coli* BL21 independently (32). Harvested cells were resuspended in 1/20 culture volume of buffer B (20 mM Tris-HCl [pH 7.9], 5 mM $MgCl_2$, 10% glycerol, 1 mM PMSF, 0.1% Nonidet P-40) containing 6 M guanidinium HCl, 500 mM KCl, and 10 mM imidazole, incubated on ice for 15 min, and then sonicated for 30 s. After centrifugation (40,000 × *g*, 30 min), the supernatant was incubated with 1/20 volume of Ni^{2+}-nitrilotriacetic acid-agarose for 30 min with rotation. After washing with the same buffer, protein was eluted with the same buffer containing 200 mM imidazole. The independently purified subunits were mixed at an equimolar ratio and dialyzed against buffer B containing 2 M guanidine-HCl and 500 mM KCl for 12 h and then dialyzed against buffer B containing 100 mM KCl for 12 h. The TFIIA complex was further purified by gel filtration using fast protein liquid chromatography (Superose 12) and the same chromatography buffer. Recombinant *S. cerevisiae* TBP was expressed in and purified from *E. coli* as described previously (32) except that trypsin cleavage of the histidine tag was omitted.

The nucleosome positioning constructs containing the adenovirus major late promoter TATA box sequence at the nucleosomal edge (+0 edge) and at the dyad (+0 dyad) have already been described (32). DNase I footprinting was done as previously described (32). Constructs which had been subcloned into pBluescript were cut with *Xba*I, labeled by using Klenow fragment and radiolabeled deoxynucleotides, and then cut with *Dde*I to liberate a 180-bp fragment. This fragment was gel purified and used to reconstitute nucleosome core particles. The assay for TBP/TFIIA binding was as described above and was scaled up as necessary. Samples were digested with DNase I at a concentration of 30 μg/ml (for octamers) or 200 ng/ml (for naked DNA) for 2 min at 30°C. The reaction was stopped with a twofold excess of EDTA, made 0.25% SDS and 0.3 M sodium acetate, and extracted with phenol and phenol-chloroform prior to precipitation. Samples were resolved on a 6% denaturing gel.

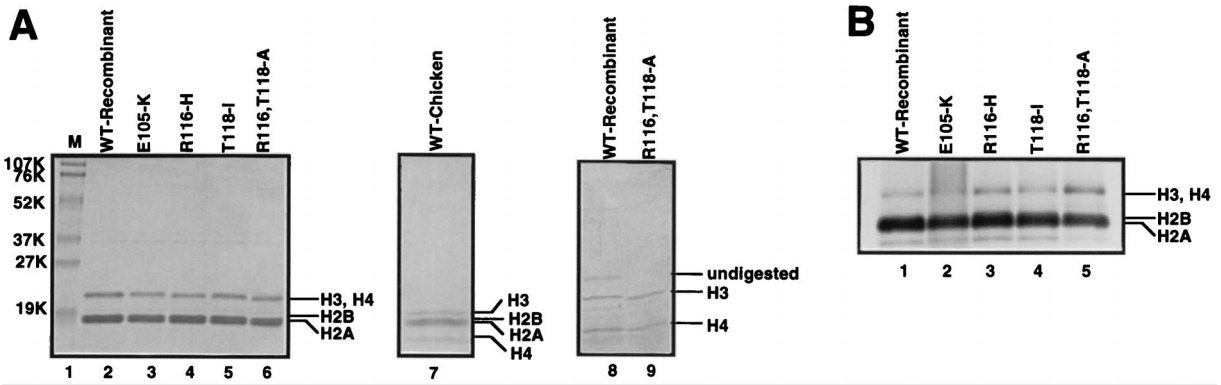

FIG. 2. Histone stoichiometry in reconstituted nucleosomes. (A) Nucleosomes were reconstituted on plasmid DNA which contains a tandem repeat of the *X. borealis* 5S RNA gene by the salt dialysis method and separated on 0.7% agarose gels. Bands corresponding to nucleosomes were excised and electroeluted. Core histones were precipitated with 20% trichloroacetic acid and analyzed by SDS–18% polyacrylamide gel electrophoresis. Proteins were visualized by silver staining (107). Lane 1, molecular weight markers (M); lanes 2 and 7, recombinant and chicken erythrocyte wild-type (WT) histones, respectively; lanes 3 to 6, nucleosomes containing histone H3 mutants E105-K, R116-H, T118-I, and R116,T118-A, respectively. Recombinant $(H3\text{-}H4)_2$ tetramers contain stoichiometric amounts of histones H3 and H4. One microgram of recombinant $(H3\text{-}H4)_2$ tetramers was treated with 3 ng of enterokinase to remove His tags and analyzed by SDS–18% polyacrylamide gel electrophoresis. Lanes 8 and 9, recombinant wild-type tetramers and tetramers containing histone H3 mutant R116,T118-A, respectively. Proteins were silver stained. (B) Nucleosomes were reconstituted on a 424-bp DNA fragment which contains a tandem repeat of the *X. borealis* 5S RNA gene by the salt dialysis method, and mononucleosomes were isolated by sucrose gradient centrifugation. Core histones from the mononucleosomal fraction were precipitated with 20% trichloroacetic acid and analyzed by SDS–18% polyacrylamide gel electrophoresis. Proteins were stained with silver. Lane 1, recombinant wild-type histones; lanes 2 to 5, nucleosomes containing histone H3 mutants E105-K, R116-H, T118-I, and R116,T118-A, respectively.

RESULTS

Influence of Sin mutants on nucleosomal structures reconstituted in vitro. Our experimental strategy (Fig. 1) was to express *Xenopus laevis* histone H3 in *E. coli* either as a wild-type protein or as a protein containing the Sin mutations (Fig. 1A). All of our recombinant proteins contain an amino acid extension at the amino terminus. We have not found such extensions to influence the efficiency of nucleosome assembly in vivo (28) or in vitro (this work). However, we are careful to compare the properties of recombinant wild-type H3 and H4 containing this N-terminal extension with that of wild-type histones H3 and H4 isolated from chicken chromatin in all of our nucleosome reconstitution experiments. The recombinant H4 contains additional amino acid sequences between the His tag and the normal protein (see Materials and Methods) that lead the recombinant H3 and H4 to comigrate on SDS–18% polyacrylamide gels (Fig. 1C, lanes 6 and 7). The recombinant histone H3 was purified (Fig. 1C; Materials and Methods) and mixed with wild-type histones H2A and H2B and recombinant H4 under denaturing conditions, and nucleosomes were reconstituted by dialysis from high salt and urea concentrations, using short DNA fragments or plasmid DNA molecules as indicated (Fig. 1D). Nucleosomes were reconstituted by using all three single-point mutations of histone H3 leading to the Sin2 phenotype (49); we also made use of an additional mutant form of histone H3 in which two amino acids whose substitution leads to a Sin phenotype were altered (R116,T118-A [Fig. 1]).

We initially examined whether histones H2A and H2B were assembled into nucleosomes containing the mutant H3 proteins. We reconstituted a plasmid DNA molecule containing a 424-bp tandem repeat of the *X. borealis* 5S RNA gene (pX5S 197-2 [87]) with core histones by the salt dialysis method (16). The reconstituted nucleosome was resolved from free histones and naked DNA on a nondenaturing 0.7% agarose gel (see Fig. 5A). The band corresponding to the minichromosome was excised and electroeluted. The histones were precipitated with 20% trichloroacetic acid and analyzed by SDS–18% polyacrylamide gel electrophoresis. The silver-stained gel reveals that the stoichiometry of histone H2A-H2B dimers to H3-H4 dimers that are assembled into nucleosome cores was equal in all reconstituted minichromosomes (Fig. 2A; compare lane 2 with lanes 3 to 6). Note that our extraction and staining protocol (107) is especially sensitive to the lysine-rich histones H2A and H2B compared to the arginine-rich histones H3 and H4; this is best shown by the staining of core histones from chicken erythrocytes that are assembled into minichromosomes and then analyzed by the same procedure (Fig. 2A, lane 7; reference 18). Other protocols give equivalent staining and recovery of all of the core histones (18); however, we needed to focus on the incorporation of H2A and H2B since it has been suggested that these proteins might be deficient in transcriptionally competent chromatin (7, 36), including nucleosomes destabilized by the SWI/SNF complex (70). We also fractionated nucleosome cores reconstituted on a 424-bp linear DNA fragment away from free DNA and free histones, using sucrose gradients (see Fig. 7B). Again an equivalent stoichiometry of histones H2A and H2B was obtained for all the reconstitutes containing mutant H3 proteins as obtained with those containing recombinant wild-type H3 (Fig. 2B). We also wished to determine that histone H3 and H4 were assembled into chromatin with appropriate stoichiometry. We assembled tetramers onto plasmid DNA molecules (36) and recovered the resulting tetramer-DNA complex before treatment with enterokinase to remove the His tags. The proteolytic products from tetramers containing wild-type recombinant H3 and a mutant H3 (R116, T118-A) are shown in Fig. 2A, lanes 8 and 9. An approximate equimolar stoichiometry of histones H3 and H4 is obtained consistent with the anticipated reconstitution process (25, 45).

We next examined the capacity of wild-type histone H3, wild-type recombinant histone H3, and mutant histone H3, together with the appropriate stoichiometries of wild-type histones H2A, H2B, and H4, to protect a DNA fragment containing the *X. borealis* somatic 5S rRNA gene from nuclease digestion (wild-type histones are those isolated from chicken erythrocytes; wild-type recombinant histones are those isolated after expression in bacteria). MNase prefers to cleave chromatin in the most accessible DNA. First the linker DNA between

nucleosomes is cut, and then the nuclease digests the rest of the linker until nucleosome core particles containing an octamer of core histones $(H2A\text{-}H2B\text{-}H3\text{-}H4)_2$ and 146 bp of DNA accumulate (63). However, the nucleosome core particle itself represents only a kinetic intermediate in the digestion of DNA. Eventually MNase can degrade the DNA in this residual structure, and the core particle will fall apart.

Our initial analysis used minichromosomes reconstituted by using an entire DNA molecule including two *Xenopus* 5S rRNA genes (pX5S 197-2) and relatively low concentrations of MNase. We find that wild-type chicken core histones reconstitute chromatin that generates a robust protection of core particle-size DNA on MNase digestion, as seen from the accumulation of DNA fragments of 146 bp in length during digestion (Fig. 3, lanes 2 and 3). However, whereas some of the minichromosomes containing the mutant histone H3 proteins also allow efficient accumulation of large amounts of core particles (E105-K [lanes 5 and 6]), others generate only a small amount of core particles (T118-I [lanes 11 and 12]) and others show little or no accumulation of core particles during MNase digestion (R116-H [lanes 8 and 9]). All of these templates had practically complete reconstitution of nucleosomes as assayed by linking number change (18 to 20 on a 3.5-kb plasmid [see Fig. 5B]). Therefore, the failure to detect core particles during MNase digestion is not apparently due to a failure to have stable interaction of histones with DNA in a nucleosome-like architecture that alters DNA topology. Care was also taken in this experiment to ensure that equivalent amounts of radioactive reconstituted nucleosomes were added to the digestion reaction in order to facilitate comparison.

Our next experiments extended this analysis by using MNase to mononucleosomes reconstituted on linear DNA fragments (238 bp) in length, which we could also use for DNase I and hydroxyl radical cleavage analysis (see Fig. 4 and 6). MNase digestion of our reconstituted mononucleosomes when either wild-type histone H3 or recombinant wild-type histone H3 is used for assembly again shows a clear kinetic intermediate in digestion of ~146 bp, reflecting the assembly of a nucleosome core particle (Fig. 3B; core particle-size DNA is indicated by the dots between lanes 3 and 4 and lanes 7 and 8) (63). However, when the double mutant of histone H3 (R116,T118-A) is incorporated, there is no substantial accumulation of material around ~146 bp; instead, there is rapid digestion of DNA to fragments smaller than 90 bp (Fig. 3B, lanes 10 to 17; the original DNA fragment of 238 bp remains visible in lanes 16 and 17, at very low levels of digestion). Although a naked DNA control is not shown in this Fig. 3B, cleavage of this 238-bp naked DNA fragment with MNase generates a series of smaller DNA fragments identical to those seen in Fig. 3B, lanes 10 to 17 (37a). Our next experiments examined the consequences of incorporating the individual Sin mutations of histone H3 into our reconstitution protocol. The accumulation of core particle-size DNA is indicated by the dots in Fig. 3C between lanes 4 and 5, 9 and 10, and 19 and 20. We find that compared to wild-type H3 (Fig. 3C, lanes 2 to 5), the Sin mutants with the exception of E105-K assemble histone-DNA complexes that appear significantly less resistant to MNase digestion. For the R116-H mutation, the nucleosome core boundary at ~146 bp is almost completely absent (Fig. 3C, lanes 12 to 15); for the T118-I mutation, there is a substantial reduction in protected DNA fragments ~146 bp in length (Fig. 3C, lanes 17 to 20); however, there are only minor reductions in stability compared to the wild type for the E105-K mutation (Fig. 3C, lanes 7 to 10). The wild-type, wild-type recombinant, E105-K, and T118-I histone H3s also show transient accumulation of a DNA fragment of ~123 bp during MNase digestion which presumably reflects a stable core histone-DNA complex smaller than the nucleosome core particle (Fig. 3B and C, arrowheads). Such subnucleosomal complexes have been observed with histone tetramers $(H3\text{-}H4)_2$ or hexamers $[H2A\text{-}H2B(H3\text{-}H4)_2]$ bound to DNA (36, 74). This intermediate in digestion is again absent in the Sin mutation R116-H and the double mutation of histone H3. These experiments lead us to suggest that the Sin mutations allow the incorporation of all of the core histones into a nucleosomal structure (Fig. 2) but that the contacts of histones with DNA are destabilized to various extents. In particular, the association of histones H2A and H2B appears to be particularly vulnerable to mutations of H3 leading to a Sin phenotype, as predicted (70). This is because H2A and H2B help define the boundaries of resistance to MNase digestion in the nucleosome core (23). If those boundaries are no longer detected upon MNase digestion (Fig. 3), then potentially H2A-H2B binding has been destabilized.

DNase I digestion of nucleosome core particles has been used to demonstrate the wrapping of DNA on the surface of the core histones (56) and the precise rotational positioning of the double helix with respect to the histone surface such that certain sequences are exposed toward solution and others make contact with the histones (79). The DNA fragment used in this work (238 bp in length) contains the *X. borealis* somatic 5S rRNA gene that can be precisely positioned with respect to the surface of the histone octamer (38, 39). DNase I cleavage of reconstituted nucleosomes containing wild-type core histones shows an alternating pattern of DNase I cleavage and protection compared to naked DNA with the cleavage sites spaced every 10 to 11 bp (Fig. 4, dots). This DNase I footprint is identical to those previously reported for the 5S rRNA gene (38, 39, 75). The precise rotational positioning of DNA on the surface of the core histones as revealed by DNase I cleavage (Fig. 4A, lane 4) is maintained in the Sin mutant E105-K (lane 5) but substantially lost in the Sin mutants T118-I (lane 5) and R116-H (lane 6) and the H3 double mutant (lane 8). We suggest that certain of the Sin mutations (R116-H and T118-1) destabilize contacts between the core histones and DNA such that rotational positioning as revealed using DNase I is substantially lost (but see Fig. 6). The H3 mutant E105-K appears to assemble a nucleosome that has stability to DNase I digestion comparable to that of a nucleosome containing wild-type recombinant H3. Taken together, our experiments with MNase (Fig. 3) and DNase I (Fig. 4) lead us to hypothesize that certain of the Sin mutations in histone H3 (R116-H and T118-I) alter the quality of histone association with DNA such that the assembled structure is much less stable. We next attempted to explore this possibility by using alternative probes of nucleosome core structure.

Each nuclease is a DNA-binding protein that can compete for histone association with DNA and disrupt weak histone-DNA contacts. Therefore, alternate strategies must be used to identify potentially unstable nucleosomes. The resolution of nucleoprotein complexes on a nondenaturing gel does not necessarily indicate nucleosome assembly, as histones can bind to DNA without the assembly of a specific structure. A simple methodology to determine the assembly of nucleosomes is to make use of the observation that the introduction of each histone octamer into association with a closed circular plasmid DNA molecule in the presence of topoisomerase I introduces one negative superhelical turn into DNA (30, 80). The introduction of one negative superhelical turn into a closed circular plasmid DNA molecule by the assembly of a single nucleosome is explained by both the wrapping of DNA around the core histones and the overwinding of the double helix in the nucleosome compared to DNA structure in solution (8, 38, 99).

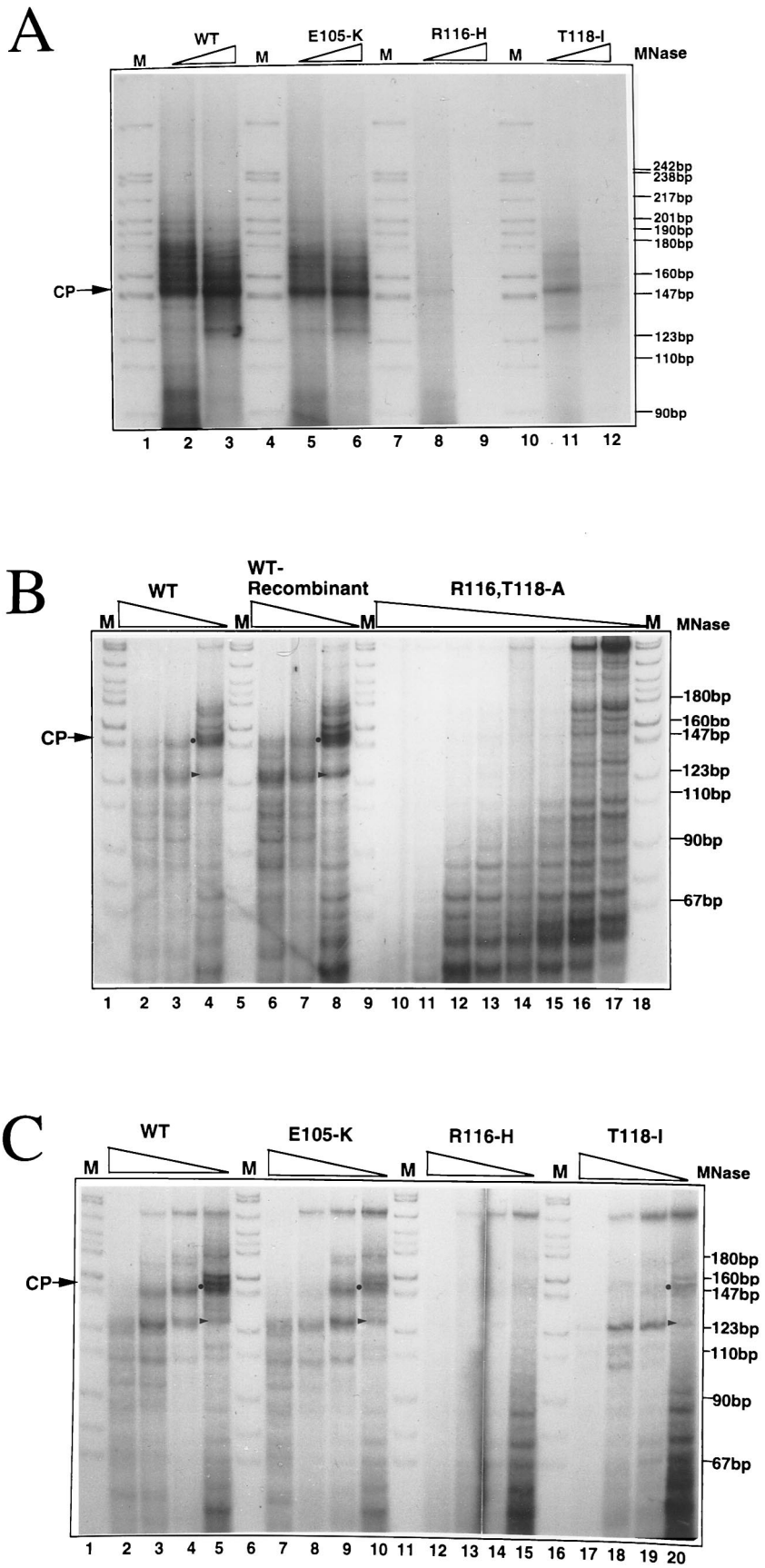
A
WT
E105-K
R116-H
T118-I
M
MNase
242bp
238bp
217bp
201bp
190bp
180bp
160bp
147bp
123bp
110bp
90bp
CP
1 2 3 4 5 6 7 8 9 10 11 12
B
WT
WT-
Recombinant
R116,T118-A
M
MNase
180bp
160bp
147bp
123bp
110bp
90bp
67bp
CP
1 2 3 4 5 6 7 8 9 10 11 12 13 14 15 16 17 18
C
WT
E105-K
R116-H
T118-I
M
MNase
180bp
160bp
147bp
123bp
110bp
90bp
67bp
CP
1 2 3 4 5 6 7 8 9 10 11 12 13 14 15 16 17 18 19 20

FIG. 3. Sin mutations of histone H3 destabilize nucleosome core particles to MNase. (A) Nucleosomes were reconstituted on plasmid DNA (pX5s 197-2) which contains a tandem repeat of the *X. borealis* (Materials and Methods) 5S RNA gene and digested with MNase. After 10 min of incubation with MNase, DNA fragments were extracted with phenol-chloroform and labeled with T4 polynucleotide kinase. ^{32}P-labeled DNA fragments were analyzed by nondenaturing 6% polyacrylamide gel electrophoresis. Lanes 1, 4, 7, and 10, *Msp*I digests of pBR322 (M); lanes 2 and 3, recombinant wild type (WT); lanes 5 and 6, E105-K; lanes 8 and 9, R116-H; lanes 11 and 12, T118-I. The amounts of MNase are 0.00025 U (lanes 2, 5, 8, and 11) and 0.0025 U (lanes 3, 6, 9, and 12). (B) DNA fragments (238 bp) that contain a single copy of 5S DNA were prepared by PCR. Core histones were incubated with the 238-bp 5S DNA fragment, and nucleosomes were reconstituted by the salt dialysis method (Materials and Methods). Reconstituted nucleosomes were digested with various amounts of MNase. After treatment of MNase, the DNA fragments were extracted by phenol-chloroform and labeled by T4 polynucleotide kinase with [γ-^{32}P]ATP. The labeled DNA fragments were separated by nondenaturing 6% polyacrylamide gel electrophoresis. Lanes 2 to 4, nucleosomes containing wild-type core histones purified from chicken erythrocytes; lanes 6 to 8, recombinant wild-type histone lanes 10 to 17, nucleosomes including the R116,T118-A mutations in histone H3. The amounts of MNase are 2 U (lanes 2, 6, and 10), 0.25 U (lanes 3, 7, and 11), 0.025 U (lanes 4, 8, and 12), 0.016 U (lane 13), 0.0125 U (lane 14), 0.01 U (lane 15), 0.0067 U (lane 16), and 0.005 U (lane 17). Lanes 1, 5, 9, and 18 are *Msp*I digests of pBR322. (C) As in panel B except that lanes 2 to 5 are wild-type nucleosomes. Lanes 7 to 10, 12 to 15, and 17 to 20 are nucleosomes which include Sin mutant histone H3 proteins, E105-K, R116-H, and T118-I, respectively. The amounts of MNase are 2 U (lanes 2, 7, 12, and 17), 0.25 U (lanes 3, 8, 13, and 18), 0.1 U (lanes 4, 9, 14, and 19), and 0.025 U (lanes 5, 10, 15, and 20). Lanes 1, 6, 11, and 16, *Msp*I digests of pBR322. The dots indicate a kinetic intermediate of ~146 bp corresponding to core particle-size DNA (CP) during MNase digestion, and the arrowheads represent an intermediate of ~123 bp that accumulates (see text for details).

The association of histones with plasmid DNA can be conveniently monitored by an agarose gel retardation assay (36), where increasing masses of wild-type or wild-type recombinant histones relative to DNA lead to a decrease in the mobility of negatively supercoiled form I DNA (Fig. 5A, upper panel, lanes 2 to 4 and 17 to 19). All of the Sin mutations of H3 form stable complexes with DNA in the presence of the other core histones (Fig. 5A, upper panel, lanes 5 to 13). However, there appears to be some dissociation of histones from DNA during electrophoresis when the double H3 mutant is used (Fig. 5A, upper panel, lane 15). Nevertheless, this must involve the dissociation of complete histone octamers because histones H2A and H2B are recovered in the same stoichiometry compared to histones H3 and H4 as nucleosomes containing wild-type H3 from this type of gel (Fig. 2A). These same samples were then deproteinized, and the capacity to supercoil DNA was assayed on an agarose gel without chloroquine (Fig. 5A, lower panel). This result indicates a progressive increase in the number of negative superhelical turns introduced into DNA as increasing masses of core histones including the Sin mutants of H3 are

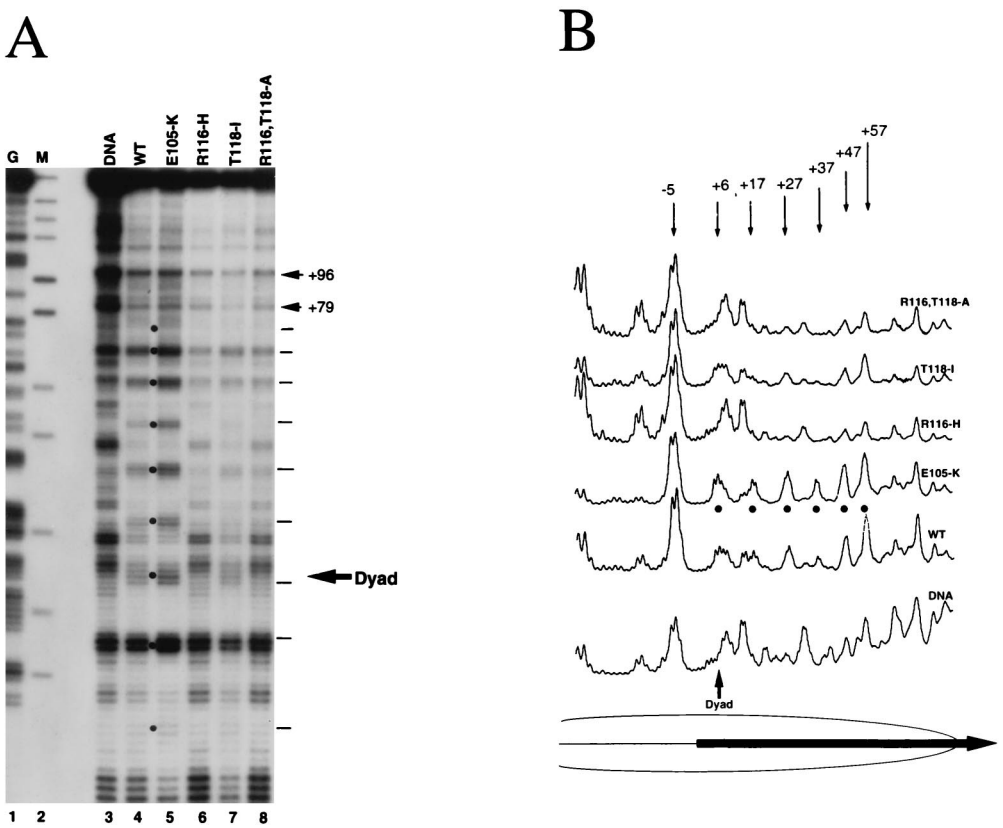

FIG. 4. DNase I footprinting of nucleosomes containing mutant histone H3 proteins. Recombinant histone H3-H4 and chicken histones H2A and H2B were incubated with 238-bp DNA fragments containing a 5S DNA to reconstitute nucleosomes (Materials and Methods). Naked DNA (95 ng) or nucleosomal DNA (400 ng) was treated with 10 or 80 ng of DNase I, respectively. The resulting DNA fragments were analyzed by denaturing 8% polyacrylamide gel electrophoresis. (A) Lanes 1 and 2, G-specific cleavage of the 5S DNA (G) and *Msp*I digests of pBR322 used as markers (M), respectively. Digestions of naked DNA (lane 3), of wild-type (WT) nucleosomes (lane 4), and of nucleosomes containing mutant histone H3 proteins (lanes 5 to 8) are shown, as indicated at the top of panel A. The large arrow indicates nucleosomal dyad; dots indicate the 10 to 11-bp spacing of DNase I cleavage sites apparent when 5S DNA is wrapped around wild-type core histones. (B) Densitometric analysis of the DNase I cleavage pattern of wild-type and mutant nucleosome core particles. The position of nucleosomal dyad and the peaks in the DNase I cleavage pattern are indicated (labeled arrows and dots). Peaks are numbered relative to the start site of transcription of the 5S RNA gene at position +1. The thick arrow is the 5S rRNA gene.

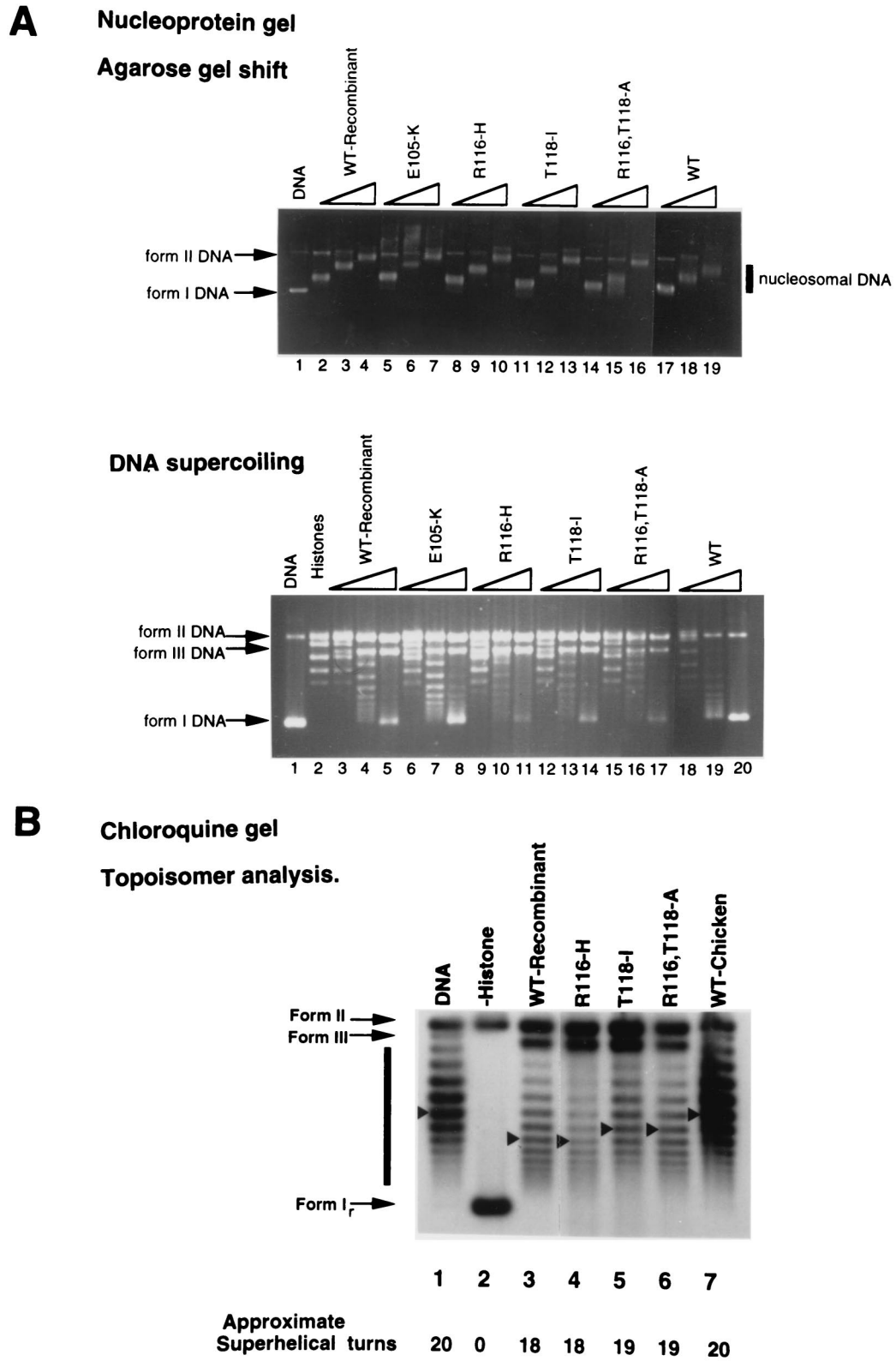

FIG. 5. Sin mutations of histone H3 do not affect nucleosome assembly on plasmid DNA. Core histones were incubated with plasmid DNA (5 μg) which contains a tandem repeat of 5S DNA (pX5S 197-2 [87]) in the presence of 2 M NaCl to reconstitute nucleosomes by the salt dialysis method. (A) Upper panel, gel shift assay. Nucleosomes were reconstituted with different amounts of core histones and separated by 1% agarose gel electrophoresis. Lane 1, plasmid DNA without core histones; lanes 2 to 4 and 17 to 19, nucleosomes with recombinant and chicken wild-type (WT) core histones, respectively; lanes 5 to 7, 8 to 10, 11 to 13, and 14 to 16, nucleosomes containing mutant histone H3 proteins E105-K, R116-H, T118-I, and R116,T118-A, respectively. The amounts of core histones used for reconstitution were 4 μg (lanes 2, 5, 8, 11, 14, and 17), 8 μg (lanes 3, 6, 9, 12, 15, and 18), and 12 μg (lanes 4, 7, 10, 13, 16, and 19), respectively. Lower panel, topological assay. Nucleosomes were treated with 2.4 U of topoisomerase I at 37°C for 30 min. Nucleosomal DNA was then extracted by phenol-chloroform, followed by 1% agarose gel electrophoresis.

reconstituted into nucleosomes. These results lead us to suggest that nucleosomes containing each of the Sin mutant H3 molecules can be assembled on closed circular plasmid DNA molecules. However, although the lower panel of Fig. 5A demonstrates that the various mutant core histone H3 molecules can be assembled into particles that introduce topological constraint, this assay does not allow us to determine how efficiently each particle constrains nucleosomes. We have made extensive use of topological assays to determine nucleosome number (18, 51, 52). To determine absolute DNA topology, it is necessary to use marker DNAs with a known number of negative superhelical turns and to count DNA topoisomers on two-dimensional agarose gels (18, 51, 52). In Fig. 5B, we show that reconstitution of equivalent masses of wild-type recombinant and mutant H3 into nucleosomes on a closed circular plasmid DNA molecule (3.5 kb in length) relative to a marker DNA of known topology leads to approximately the same number of negative superhelical turns (18 to 20) being introduced in the presence of topoisomerase I (Fig. 5B; compare lanes 3 to 7). This corresponds to one nucleosome core every 175 to 194 bp. We conclude that all of the recombinant H3 molecules have the capacity to be assembled into nucleosome cores that wrap DNA comparably to wild-type core histones.

The helical periodicity of DNA on the surface of the histone octamer is conveniently assayed by using the hydroxyl radical as a DNA cleavage reagent. The hydroxyl radical is generated by chemistry that does not require any contact with the double helix (86). Cleavage of the DNA molecule varies dependent on the width of the minor groove and on protein association (13, 40). Importantly, the hydroxyl radical is a noninvasive probe of DNA structure in the nucleosome and has been shown to detect histone-DNA contacts that are not revealed by DNase I digestion (38, 39, 71). Hydroxyl radical cleavage of reconstituted histone-DNA complexes containing the Sin mutants of H3 reveal that DNA is wrapped around the histones with a unique rotational position in all instances (Fig. 6). This result is in marked contrast to that obtained with DNase I (Fig. 4). We believe that the reason for this difference is the necessity for DNase I to bind to DNA and hence compete with the histones for association with DNA before cleaving it. The hydroxyl radical has no need to form a stable complex with DNA before the cleavage reaction; therefore, it is much less disruptive of histone-DNA interactions. Wild-type and recombinant histone H3 direct the assembly of identical nucleosomal structures (Fig. 6A; compare lanes 4 and 5). The Sin mutations T118-I and E105-K lead to the assembly of nucleosomes with wrapping of DNA very similar to that observed with the wild-type histone H3 (Fig. 6A; compare lanes 1, 3, 4, and 5). The precise helical periodicity of the double helix on the surface of the histone octamer as revealed by hydroxyl radical cleavage is like that previously observed both for 5S rRNA gene containing nucleosomes and mixed-sequence nucleosomes (the numbers refer to base pair positions relative to the start site of 5S rRNA gene transcription, +1 [38, 39]). However, the R116-H mutant wraps DNA, but with a rotational positioning of the double helix relative to the histone surface that is shifted by 1 to 2 bp relative to nucleosomes containing the wild type or other Sin mutants of histone H3 (Fig. 6A; compare lane 2 with lanes 1, 3, 4, and 5). The shift in rotational positioning of DNA is more apparent in the densitometric scans of the hydroxyl radical cleavage pattern (Fig. 6B; compare positions of peaks indicated with arrowheads, which are for wild-type histones with those indicated with dots, which are for the R116-H mutant). A second difference between the Sin mutant R116-H and the other Sin mutants and wild-type H3 is that nucleosomes containing this protein show a much less extended modulation of hydroxyl radical cleavage toward the periphery of the nucleosome (Fig. 6B; compare scans of the wild type and R116-H [black bar]). This portion of nucleosomal DNA is still partially constrained on a histone surface because modulations in radical cleavage exist; however, the cleavage pattern is much more like that of naked DNA. Earlier work has shown that this region of the 5S rRNA gene makes contacts with histones H2A and H2B (Fig. 6C and D; references 39 and 71). In the R116-H mutant nucleosome, the quantitative modulations of hydroxyl radical cleavage over the three turns of DNA to either side of the dyad axis are very similar to those of wild-type nucleosomes. Thus, although the region of DNA actually in contact with the Sin mutant histone H3 is wrapped in a manner similar to that observed in the wild-type nucleosome, the main region of quantitative variation in hydroxyl radical cleavage occurs in a different region of the nucleosome (see Discussion). To control for the contacts of core histone with the DNA in the various reconstitutions shown in Fig. 6A and B, we reconstituted the same DNA fragment with an intact histone octamer [$(H2A\text{-}H2B\text{-}H3\text{-}H4)_2$ (Fig. 6C, lane 3)], with a histone tetramer [$(H3\text{-}H4)_2$ (Fig. 6C, lane 4)], and with histone H2A-H2B dimers (Fig. 6C, lane 5). Compared to naked DNA, the DNA associated with the H2A-H2B dimers shows no changes in hydroxyl radical cleavage (Fig. 6C; compare lanes 2 and 5); however, the other histone-DNA complexes show changes (compare lane 2 with lanes 3 and 4). Densitometric scans of these gel lanes are shown in Fig. 6D. The modulation of hydroxyl radical cleavage extends into the entire TFIIIA binding site (+45 to +95) with the histone octamer $(H2A\text{-}H2B\text{-}H3\text{-}H4)_2$ but not with the histone tetramer $(H3\text{-}H4)_2$. This is consistent with histones H2A and H2B making contact with DNA in the +67 to +95 region of this DNA fragment (72).

The results of our topological and hydroxyl radical cleavage analyses indicate that the Sin histone H3 mutants are incorporated into nucleosomal structures. The topological constraints are similar whether wild-type or mutant H3 is present (Fig. 5); moreover, 5S DNA is actually wrapped on the surface of the histones with a defined rotational position (Fig. 6). This difference in result from that obtained with DNase I as a probe (Fig. 3) might be explained by the fact that the hydroxyl radical does not need to form a stable nucleoprotein complex with nucleosomal DNA before DNA cleavage can occur (see Discussion). For the R116-H Sin mutant, hydroxyl radical cleavage reveals variation in the constraint of DNA at the edge of the nucleosome core (Fig. 6B). We conclude that the alterations in nuclease accessibility (Fig. 3 and 4) are not due to a failure to assemble nucleosomes per se but are instead due to

Lanes 1 and 2, untreated and topoisomerase I-treated naked plasmid DNA, respectively; lanes 3 to 5 and 18 to 20, nucleosomes reconstituted with recombinant and chicken wild-type core histones, respectively; lanes 6 to 8, 9 to 11, 12 to 14, and 15 to 17, nucleosomes containing mutant histone H3 proteins E105-K, R116-H, T118-I, and R116,T118-A, respectively. (B) Nucleosomes were reconstituted on plasmid DNA which contains a tandem repeat of the *X. borealis* 5S RNA gene by the salt dialysis method and treated with topoisomerase I. Topoisomers were separated on a 1.0% agarose gel containing 90 μg of chloroquine per ml and detected by Southern hybridization. Lane 1, negatively supercoiled DNA known to contain an average of 20 negative superhelical turns (18); lane 2, closed circular DNA which is relaxed by topoisomerase I; lanes 3 and 8, recombinant and chicken erythrocyte wild-type histones, respectively; lanes 4 to 7, E105-K, R116-H, T118-I, and R116,T118-A, respectively. The average number of nucleosomes reconstituted is indicated below each lane.

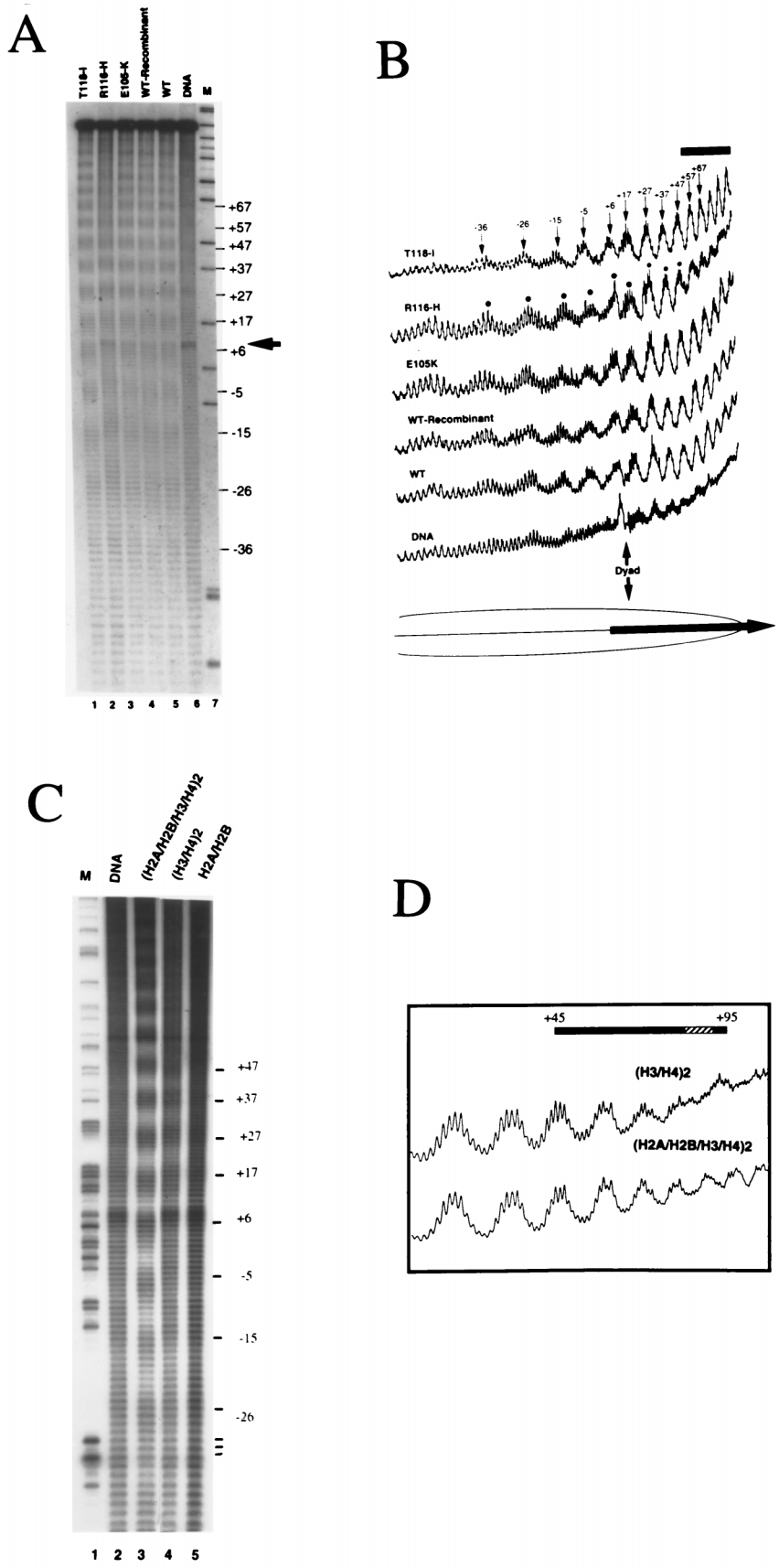
A
T118-I
R116-H
E105-K
WT-Recombinant
WT
DNA
M
+67
+57
+47
+37
+27
+17
+6
-5
-15
-26
-36
1 2 3 4 5 6 7
B
-36
-26
-15
-5
+6
+17
+27
+37
+47
+57
+67
T118-I
R116-H
E105K
WT-Recombinant
WT
DNA
Dyad
C
M
DNA
(H2A/H2B/H3/H4)2
(H3/H4)2
H2A/H2B
+47
+37
+27
+17
+6
-5
-15
-26
1 2 3 4 5
D
+45
+95
(H3/H4)2
(H2A/H2B/H3/H4)2

FIG. 6. Hydroxyl radical footprints of nucleosome core particles that include Sin mutant histone H3 proteins. Mononucleosomes were reconstituted and used for hydroxyl radical footprinting as described in Materials and Methods. Nucleosomal DNAs were isolated and analyzed by denaturing 8% polyacrylamide gel electrophoresis. (A) Autoradiograph of DNA fragments generated by hydroxyl radical cleavage. Lanes 1 to 3, footprints of nucleosomes containing mutant histone H3 proteins T118-I, R116-H, and E105-, respectively; lanes 4 and 5, footprints of nucleosomes containing wild-type (WT) recombinant and chicken histones, respectively; lane 6, naked DNA; lane 7, *Msp*I digest of pBR322 (M). (B) Densitometric analysis of the hydroxyl radical cleavage pattern of wild-type and mutant core particles. The position of nucleosomal dyad and the peaks in the DNase I cleavage pattern are indicated (arrowheads for all scans except the dots for R116-H). Peaks are numbered relative to the start site of transcription of the 5S RNA gene at position +1. Thick arrow is 5S RNA gene; the thick bar above the scans indicates the region of reduced modulation of hydroxyl radical cleavage for the R116-H Sin mutant. (C and D) As in panels A and B except that wild-type chicken core histones were used to reconstitute distinct histone-DNA complexes. (C) Hydroxyl radical cleavage of naked DNA (lane 2) and cleavage of DNA associated with either a complete histone octamer (lane 3), a histone tetramer (lane 4), or histone dimers (lane 5) bound to the 5S DNA. (D) Densitometer scans of selected lanes of hydroxyl radical cleavage patterns of 5S DNA bound by either a histone octamer or a histone tetramer as indicated. The locations of the TFIIIA binding site and the most important region for contacts to DNA by TFIIIA are indicated by a solid bar and a hatched box, respectively.

alterations in the stability with which the core histones constrain DNA in the presence of the Sin mutants of histone H3.

Influence of Sin mutants on the structural and functional properties of a dinucleosome transcription template. The alterations in accessibility of the mononucleosomal structures incorporating the Sin mutants R116-H and T118-I of histone H3 to MNase and DNase I are consistent with the in vitro activities of the SWI/SNF complex and related proteins (15, 20,

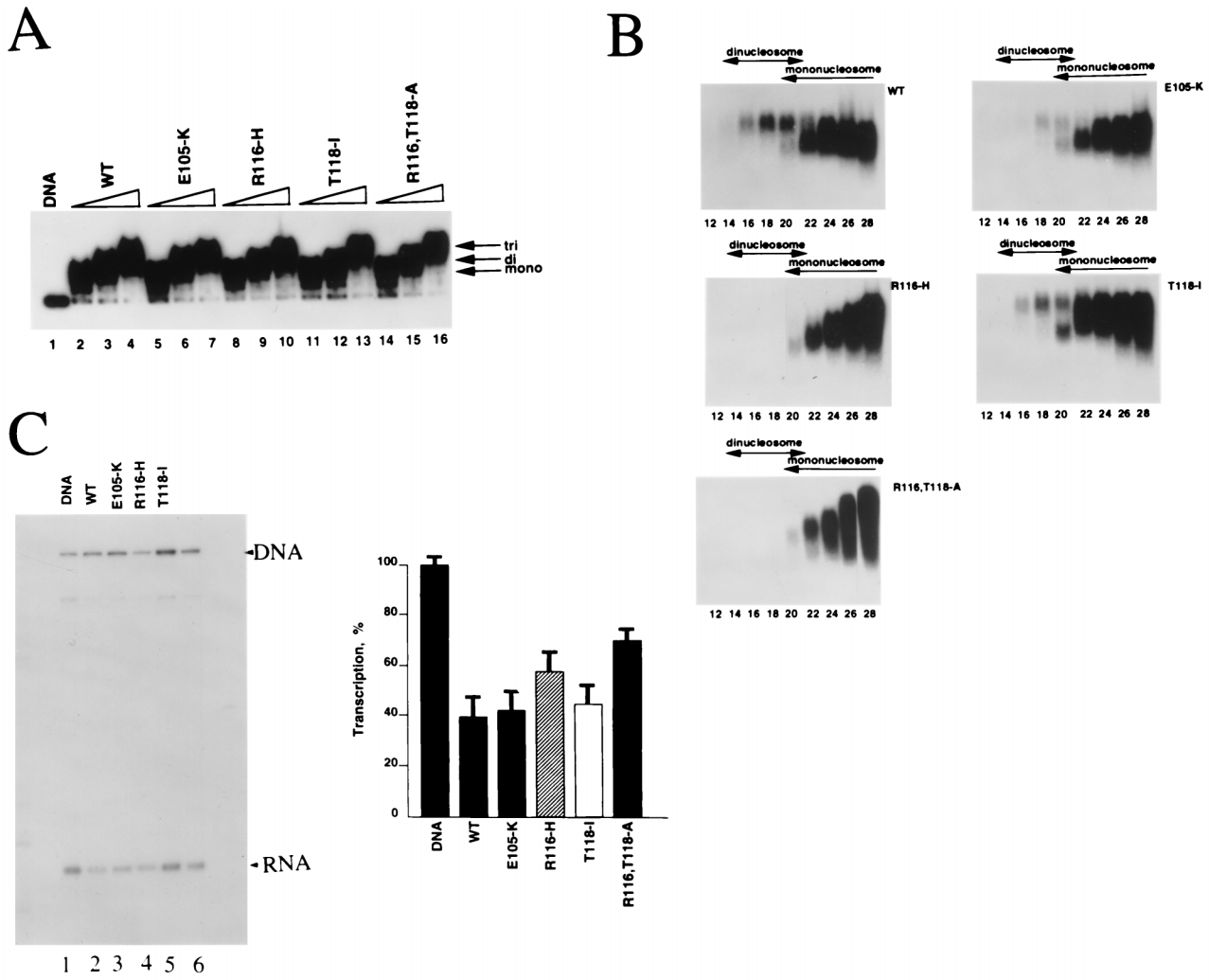

FIG. 7. Influence of Sin mutation of histone H3 on nucleosome mobility and transcription of nucleosomal templates. (A) Gel shift assay. A DNA fragment (424 bp) which contain a tandem repeat of 5S DNA was prepared from plasmid DNA (pX5S 197-2) by *Xba*I and *Xho*I digestion. Nucleosomes were reconstituted with *Xba*I-*Xho*I fragments (5 μg) and various amounts of core histones (5, 7.5, and 10 μg) by the salt dialysis method and analyzed by 0.7% agarose gel electrophoresis. Lane 1, naked DNA; lanes 2 to 4, nucleosomes containing recombinant wild-type (WT) histones H3 and H4; lanes 5 to 7, 8 to 10, 11 to 13, and 14 to 16, nucleosomes containing mutant histone H3 proteins E105-K, R116-H, T118-I, and R116,T118-A, respectively. (B) Reconstituted nucleosomes such that one histone octamer should bind per 180 bp were subjected to 5 to 20% sucrose gradient centrifugation for 19 h at 4°C. The fractions were analyzed by 0.7% agarose gel electrophoresis. The numbers below the panels indicate fraction numbers from the bottom of the gradient. (C) Nucleosomes were reconstituted with the *Xba*I-*Xho*I fragments. Nucleosomal samples were used as templates for transcription in an extract from *Xenopus* oocyte nuclei. Transcripts were analyzed by denaturating 6% polyacrylamide gel electrophoresis and quantitated with a PhosphorImager. Lane 1, transcription from naked DNA; lanes 2 to 6, transcriptions from nucleosomal DNAs which contain wild-type protein and mutant histone H3 proteins E105-K, R116-H, T118-I, and R116,T118-A, respectively. The data are shown as a bar graph, using radiolabeled DNA as an internal control. Error bars are shown. The transcriptional activity of the naked DNA template is taken as 100%.

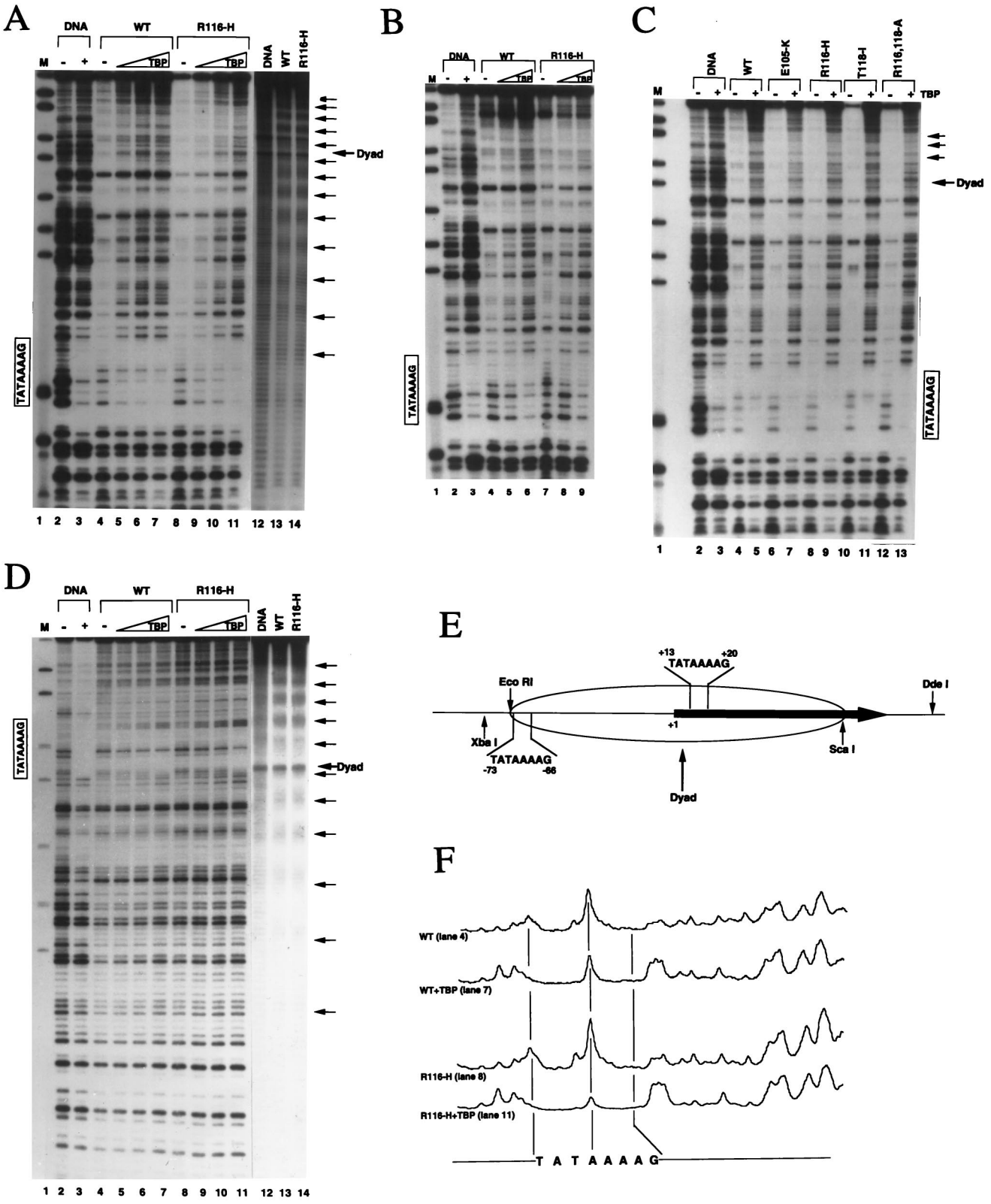

FIG. 8. DNase I footprinting of TBP/TFIIA interaction with nucleosomal DNA. DNA fragments that include a TATA box at position −73 or +13 relative to the start site of transcription of the 5S RNA gene at position +1 were prepared by *Xba*I-*Sca*I digestion of the plasmid DNA p5S (+0 edge) and p5S (+0 dyad) (32) (E). The *Xba*I site was labeled by the Klenow fragment, and the aforementioned fragment of 180 bp used as a substrate for nucleosome reconstitution. Then 200 ng of nucleosomes containing 1.6 nM labeled DNA was incubated with various amounts of TBP (100, 200, and 400 nM) in the presence of stoichiometric amounts of TFIIA. After 10 min of incubation at 30°C, samples were treated with 80 ng of DNase I for 2 min at 30°C (unless indicated otherwise), and nucleosomal DNAs were extracted by phenol-chloroform. Purified DNA samples were separated by denaturating 8% polyacrylamide gel electrophoresis. (A) DNase I footprinting of TBP interaction with

50, 84, 85). SWI/SNF directs the loss of rotational positioning of DNA on the nucleosome surface as detected using DNase I in vitro, and in vivo results indicate a role for SWI/SNF in increasing MNase access to nucleosomal DNA (42). These two effects are associated with an increase in transcription factor access to nucleosomal DNA (20, 50, 85). We next investigated whether the incorporation of the Sin mutants of H3 into a defined dinucleosomal template would relieve basal transcriptional repression. We made use of the transcriptional machinery for RNA polymerase III, because there is no known targeting of chromatin disruption directed by transcription factors required for 5S rRNA gene transcription (103). This is in contrast to the situation with the RNA polymerase II transcriptional machinery, where $TAF_{II}250$ has acetyltransferase activity (59).

Two tandemly reiterated *X. borealis* somatic 5S rRNA genes were used to define the structural properties of a dinucleosomal template and to examine the functional consequences of the assembly of different nucleosomal structures. In earlier work, we have defined the repression of 5S rRNA gene transcription due to core histones alone (87), the repression due to the incorporation of histone H1, HMG1, and other types of linker histone into the nucleosome (87, 88), and the consequences for transcription of acetylating the core histones in the presence or absence of H1 (89). Our experimental strategy to examine the effects of the Sin mutant forms of H3 was to reconstitute the 424-bp DNA fragment containing the two 5S rRNA genes with increasing masses of core histones (including the mutant H3). Agarose gel retardation experiments indicated the assembly of mixtures of mono-, di-, and trinucleosomes (Fig. 7A). Comparable levels of histone-DNA association were obtained for all Sin mutants, the H3 double mutant, and wild-type core histones. We next attempted to resolve a homogeneous population of dinucleosomes from mononucleosomes on sucrose gradients before using these as templates for in vitro transcription reactions (Fig. 7B; reference 87). Although this can be successfully achieved for the wild-type histones (Fig. 7B, wild type, fractions 16 and 18), we failed for all preparations of dinucleosomes containing mutant H3 except for T118-I (Fig. 7B, T118-I). The failure to recover assembled dinucleosomes with most of the H3 mutants is currently not understood. As discussed below, we have excluded differences in mobility or translational position of the histone octamer relative to DNA sequence as an explanation. Since we could not use our established approach (87, 89), our next experiment then focused on samples that were predominantly mononucleosomal (Fig. 7A, lanes 2, 5, 8, 11, and 14) but that also contained a small quantity of dinucleosomes.

We examined whether the histone octamers reconstituted with the wild type, the Sin mutant R116-H, or the H3 double mutant R116,T118-A had similar positioning and mobility on the 424-bp DNA fragment. Histone octamers alone can adopt a number of translational positions along a DNA sequence spaced by helical turns of DNA (i.e., 10- to 11-bp intervals) (23, 57). Bradbury and colleagues have determined, using two-dimensional nucleoprotein electrophoresis, that this spacing is also indicative of mobile nucleosomes (58). To assess nucleosome positioning and mobility, we made use of the differential resolution of nucleoprotein complexes on nondenaturing polyacrylamide gels dependent on the conformation of the histone-DNA complex (58). A single histone octamer associated with a 424-bp DNA fragment can be resolved into multiple complexes on a single dimension of electrophoresis dependent on the translational position of the histone octamer along the DNA fragment. These different translational positions were comparable for all three types of mononucleosomes containing either the wild type, Sin mutant R116-H, or the H3 double mutant R116,T118-A (data not shown). If the octamer changes position during a 1-h incubation at 4 or 37°C prior to a second dimension of electrophoresis, then this will be detected by the appearance of a nucleoprotein complex that migrates at a position away from a simple diagonal. If no mobility occurs, everything will remain on the diagonal between the common point of origin of electrophoresis for both first and second dimensions and naked DNA. Nucleosome mobility is temperature dependent; more nucleoprotein complexes migrate off the diagonal at 37°C than at 4°C. In fact, under the conditions used in our experiment, practically all of the complexes migrate off the diagonal. Both the Sin mutant R116-H and the H3 double mutant assemble mononucleosomes which are similar in positioning and mobility to wild-type nucleosomes on the 5S DNA fragment (data not shown).

Finally, we used these nucleosome preparations to examine the efficiency with which 5S rRNA gene transcription was repressed. The assembly of the 424-bp DNA fragment into a mononucleosome by using wild-type histones will repress transcription relative to naked DNA by approximately 50% (Fig. 7C; references 87 and 89). We find that the inclusion of the Sin mutants or of the double mutant of H3 leads to a moderate relief of transcriptional repression to 75% of full transcription levels at best for the double mutant R116,T118-A (the histogram shows 5S RNA levels relative to 5S DNA input). Therefore, the Sin mutants do not in isolation completely relieve core histone-mediated transcriptional repression of RNA polymerase III transcription.

Influence of Sin mutants on the access of TBP/TFIIA to the TATA box within a positioned nucleosome. In earlier work, we (32) and others (43) have investigated the influence of nucleo-

nucleosomes containing the TATA box at the edge (−73). Lane 1, *Msp*I digest of pBR322 (M); lanes 2 and 3, naked DNA without and with TBP/TFIIA, respectively; lanes 4 to 7 and 8 to 11, are wild-type (WT) nucleosomes and nucleosomes containing mutant histone H3 (R116-H), respectively. Concentrations of TBP/TFIIA are 0 nM (lanes 4 and 8), 100 nM (lanes 5 and 9), 200 nM (lanes 6 and 10), and 400 nM (lanes 7 and 11). Lanes 12 to 14, footprints of hydroxyl radical cleavage of the nucleosomes used in this study. Arrows indicate the peaks of hydroxy radical cleavage, and the bold arrow indicates nucleosomal dyad. (B) Lanes 1 to 3 are as in panel A; lanes 4 to 6 and 7 to 9 show footprinting of TBP/TFIIA bound to wild-type nucleosome and nucleosomes containing mutant histone H3 (R116-H). Concentrations of TBP/TFIIA are 0 nM (lanes 4 and 7), 100 nM (lanes 5 and 8), and 200 nM (lanes 6 and 9). The concentration of DNase I is half of that used for panel A (i.e., 40 ng of DNase I for 2 min at 30°C). (C) DNase I footprinting of TBP/TFIIA interaction with nucleosomes containing Sin mutant histone H3 proteins. DNA fragments were the same as panel A, and nucleosomes were reconstituted with mutant histone H3 proteins. Lane 1, *Msp*I digest of pBR322; lanes 2 and 4, DNase I cleavage patterns of naked DNA and wild-type nucleosomes, respectively; lanes 6, 8, 10, and 12, nucleosomes containing histone H3 mutants E105-K, R116-H, T118-I, and R116,T118-A, respectively; lanes 3, 5, 7, 9, 11, and 13, DNase I cleavage patterns of naked DNA, wild-type nucleosomes, and E105-K, R116-H, T118-I, and R116,T118-A nucleosomes in the presence of TBP (400 nM). (D) DNase I footprinting of TBP/TFIIA interaction with nucleosomes containing TATA box at the nucleosomal dyad (+13). Lane 1, *Msp*I digest of pBR322; lanes 2 and 3, naked DNA without and with TBP/TFIIA, respectively; lanes 4 to 7 and 8 to 11, wild-type nucleosomes and nucleosomes containing mutant histone H3 (R116-H), respectively. Concentrations of TBP/TFIIA are 0 nM (lanes 4 and 8), 100 nM (lanes 5 and 9), 200 nM (lanes 6 and 10), and 500 nM (lanes 7 and 11). Lanes 12 to 14, footprints of hydroxyl radical cleavage of the nucleosomes used in this study. Arrows indicate the peaks of hydroxyl radical cleavage, and the bold arrow indicates nucleosomal dyad. (E) Locations of TATA baxes and sites for restriction endonucleases relative to the 5S DNA. The ellipse indicates a position of the nucleosome, and the thick arrow indicates 5S DNA. (F) Densitometric scans of the indicated gel lanes from panel D in the vicinity of the TATA box positioned at the nucleosomal dyad.

some assembly and histone modification on the binding of TBP/TFIIA to nucleosomal DNA. TBP/TFIIA would not bind to nucleosomal DNA in a wide range of translational and rotational settings of DNA relative to the histone octamer, if the histones were unmodified and no other activities were present. TBP/TFIIA could bind to the TATA box within a nucleosome in the presence of the mammalian SWI/SNF complex if the TATA box was present in one defined rotational and translational position relative to the dyad axis of the nucleosome (43). This exact position was also reported to allow TBP/TFIIA to bind if the core histones were hyperacetylated (43). The requirement for precise rotational positioning is surprising considering that SWI/SNF treatment causes a loss of rotational positioning of DNA in the presence of DNase I (20, 43, 50). However, as we have shown, DNase I cleavage does not necessarily reveal rotationally positioned DNA, because it has the capacity to potentially disrupt that organization (compare Fig. 4 and 6). Removal of the histone tails using trypsin did not allow TBP/TFIIA association with the TATA box within a nucleosome at any rotational or translational position (32). Normally tryptic removal of the histone tails improves transcription factor access to nucleosomal DNA in a very similar way to histone hyperacetylation (55, 91, 92).

We assembled the TATA box into a positioned nucleosome at two different translational positions at the very edge and at the dyad axis (Fig. 8E). We have described the assays for translational positioning of the histone octamer with respect to DNA sequence in earlier work (32). Nucleosomes were assembled by using either wild-type histones, the Sin mutants, or the H3 double mutant. Hydroxyl radical cleavage was used to confirm nucleosome assembly (Fig. 8A, lanes 12 to 14; Fig. 8D, lanes 12 to 14). We then made use of the DNase I footprinting methodology and elevated TBP/TFIIA concentrations (43) to assay the access of TBP/TFIIA to nucleosomal DNA (Fig. 8A and B). Note that these conditions do not allow resolution of nucleoprotein complexes by gel shift methodologies. These high concentrations allow TBP/TFIIA to partially overcome repressive influences of the core histone tails on binding to nucleosomal DNA at the very edge of the nucleosome (reference 32; Fig. 8A and B). This could be due either to TBP displacing histones from the octamer surface or to a change in translational positioning of the histone octamer with respect to DNA sequence. We do not distinguish between these two possibilities here. We find that for the wild-type histone H3, the Sin mutants of histone H3, and the H3 double mutant, TBP/TFIIA can bind to nucleosomal DNA under these conditions at the very edge of the nucleosome with comparable efficiencies (Fig. 8A to C [different levels of DNase I digestion were used]). The binding of TBP/TFIIA is also reduced to comparable extents when the TATA box is close to the dyad axis (Fig. 8D and E). Densitometric scanning of wild-type nucleosomal DNA in the absence or presence of TBP/TFIIA (Fig. 8D, lanes 4 and 7; Fig. 8F, two upper scans) suggests a low level of occupancy (<30%); however, for nucleosomes containing the Sin mutant R116-H, the binding of TBP/TFIIA appears slightly improved (Fig. 8D, lanes 8 and 11; Fig. 8F, two lower scans). Nevertheless, for nucleosomes containing either wild-type or Sin mutant histone H3, the binding of TBP/TFIIA at the dyad axis of the nucleosome remains much reduced compared to naked DNA (Fig. 8D, lanes 2 and 3). Therefore, we detect only minor differences in transcription factor accessibility to DNA in nucleosomes containing the recombinant wild type or Sin mutations in histone H3, using these purified components in vitro.

DISCUSSION

The major conclusions from our work are that the Sin mutants R116-H and T118-I assemble nucleosomes that have an increased sensitivity to MNase (Fig. 3) and an altered sensitivity to DNase I cleavage (Fig. 4). These observations are consistent with the hypothesis that mutations in histone H3 leading to a Sin phenotype in yeast lead to nucleosome destabilization (49, 70, 102). However, other Sin mutants (E106-K) show little change in cleavage by DNase I and MNase following assembly into nucleosome cores. Thus, additional molecular mechanisms aside from direct nucleosome destabilization might contribute to SWI/SNF independence. Our results indicate that although nucleosomal structures might assemble in the presence of the Sin mutants of histone H3 (Fig. 2, 5, and 6), the quality of histone-DNA interactions can be changed to a variable extent, potentially over the entire nucleosome core. These changes are insufficient in isolation to strongly facilitate TBP/TFIIA binding to the TATA box at the dyad axis of a positioned nucleosome (Fig. 8) or to completely alleviate the transcriptional repression of nucleosomal templates (Fig. 7). We suggest that other activities or events will be necessary to further disrupt repressive histone-DNA interactions in order for the SWI/SNF complex to facilitate recruitment of TBP/TFIIA to the TATA box. These subsequent events might be facilitated by certain of the Sin mutations such as E105-K to a greater extent than others. The Sin mutations that create nucleosomes with enhanced sensitivity to MNase and DNase I (R116-H and T118-I) might labilize histone-DNA interactions in a general manner in order to facilitate the activity of other chromatin-disruptive agents, such as RNA polymerase II (29). Alternative targeted histone acetylation might further facilitate chromatin disruption by SWI/SNF (12). Future experiments will explore this possibility.

Sin mutations of histone H3 and chromatin structure. The Sin mutations of histone H3 cluster in the vicinity of one β-bridge motif in the H3-H4 heterodimer (49). Due to the juxtaposition of two H3-H4 heterodimers at the dyad axis of the nucleosome (3, 4), the Sin mutations might be predicted to disrupt histone-DNA interactions involving the central turn of DNA at the dyad axis. However, whereas the assembly of nucleosomes and the wrapping of DNA at the dyad axis of the nucleosome are very similar in the presence or absence of the Sin mutants of H3 (Fig. 5 and 6), in the presence of particular Sin2 mutants, MNase readily digests DNA inside the nucleosome core (Fig. 3) and DNase I disrupts rotational positioning of DNA over most of the nucleosome core (compare Fig. 4 and 6). Therefore, the observed transitions in nuclease sensitivity can occur far from the dyad axis. How might this be accomplished?

The nucleosome core is held together by extensive protein-protein and protein-DNA interactions; however, the integrity of certain interactions is more important to the overall structure than the integrity of others. The nucleosome has a central kernel of two H3-H4 heterodimers that form a stable tetramer (16). These are the first histones to be sequestered onto DNA during nucleosome assembly in vivo (106), and it is not until 120 bp of DNA is wrapped around the tetramer that two (H2A-H2B) heterodimers can associate (37). The tetramer recognizes intrinsic DNA structural features that direct nucleosome positioning, and it makes contacts with DNA that are remarkably resistant to physical perturbation (6, 22, 39). It is also important to note that DNA at the very edge of the nucleosome core might also be constrained by contacts with the fourth N-terminal α-helix of histone H3 (71). Therefore, the $(H3\text{-}H4)_2$ tetramer might have the potential to associate

with DNA at the entry and exit points of wrapping around the histone octamer and directly influence the association of histones H2A and H2B (74). Thus, the Sin mutations in histone H3 might influence H2A-H2B sequestration, nucleosome positioning, and the stability with which the $(H3\text{-}H4)_2$ tetramer binds to DNA. Destabilization of histone H3-H4 interaction with DNA at one point on the protein ramp on which DNA is wound might have transmissible effects over the entire nucleosome core. Consistent with this proposal, the R116-H mutant leads to the assembly of nucleosomes with minor changes in DNA wrapping around the dyad axis, but with more significant changes in the modulation of hydroxyl radical cleavage at the periphery of the nucleosome, in the region known to be bound by H2A and H2B (Fig. 6; reference 39).

Our results have interesting similarities to and differences from an in vivo study by Wechser et al. (98) on the structural consequences of Sin mutations of H4. These investigators noted that the histone H4 mutants that give a Sin phenotype cause an increase in the accessibility of chromatin to Dam methyltransferase and MNase. Our results with MNase, indicating increased access to nucleosomal DNA when the H3 mutants are assembled into nucleosomes in vitro are in agreement with this conclusion (Fig. 3). Wechser et al. also concluded that their H4 mutants were competent for nucleosome assembly, but that the capacity of nucleosomes to constrain supercoils in vivo was greatly reduced. We also observe nucleosome assembly in assays using the H3 mutant in vitro (Fig. 6) and find that these nucleosomes constrain DNA comparably to wild-type histones (Fig. 5B). The difference in topological constraint of DNA within nucleosomes containing Sin mutant core histones observed between our studies and those of Wechser et al. might be due to the presence of additional activities that can destabilize nucleosomes in the yeast nucleus, or they might be due to additional sequence differences between yeast and metazoan core histones. An important point is that there is substantial variation in the structural consequences for nucleosomes in vitro of incorporating particular mutants of H3 that generate a Sin phenotype. Thus, differences between Sin mutant forms of H3 and H4 might be anticipated.

Sin mutations, SWI/SNF activity, and the transcription process. The exact mechanisms by which the SWI/SNF complex activates transcription remain unknown. The connection to chromatin derives from the isolation of suppressors of mutations of SWI/SNF components in yeast. These suppressors include the gene *SPT6* (62) mutations which are similar in phenotype to mutations in H2A and H2B (19, 26), the gene *SIN1*, which encodes a small hydrophilic HMG1 like protein (48), and mutations in the genes for histones H3 and H4 (49). Components of the SWI/SNF complex are important in directing alterations in chromatin structure around the upstream activation sequence region and the TATA box of the *SUC2* promoter that are independent of transcription itself (42). It was further suggested that the SWI/SNF activators function by removing or otherwise modifying nucleosomes to increase accessibility of the TATA box to TFIID. Consistent with this hypothesis, nucleosomes assembled in vitro by using metazoan histones can be disrupted by either the yeast SWI/SNF (20) or related metazoan (43, 50) complexes. TBP/TFIIA can bind to nucleosomal DNA at the dyad axis of the nucleosome core in the presence of SWI/SNF (43). We find that the Sin mutations of H3 assemble nucleosomes that wrap DNA at the dyad axis like wild-type core histones; however, in certain mutants (R116-H and T118-I), this constraint does not prevent DNase I cutting nucleosomal DNA in a manner very similar to cleavage of naked DNA. Therefore, it is possible that DNase I can displace DNA very easily from the dyad axis of certain nucleosomes containing Sin mutants of H3. However, we find only a weak facilitation of TBP/TFIIA binding to DNA at the dyad axis of the nucleosome following inclusion of Sin mutants of H3 (Fig. 8D and F). We suggest that other activities, for example, the RNA polymerase II holoenzyme or coactivator complex (5, 12, 29), might be important in further facilitating the association of the basal transcriptional machinery including TBP with a nucleosomal template.

In humans, two proteins with homology to SWI/SNF components are hbrm (or hSNF2α) and BRG1 (or hSNF2β); these proteins possess amino-terminal proline- and glutamine-rich regions which resemble transcriptional activation domains, while the carboxyl-terminal regions contain a conserved bromodomain (47, 60, 61). The capacity of these proteins to interact with other components of the transcriptional machinery is shown by their capacity to activate transcription by transient cotransfection assays that are largely independent of chromatin-mediated effects (47, 61). The human BRG1 protein can immunoprecipitate with antibodies against p300/CBP, and p300/CBP can immunoprecipitate with $TAF_{II}250$ (21). Therefore, it is probable that histone acetyltransferases will also contribute to chromatin disruption (12, 64, 108). Consistent with this possibility, a distinct class of Sin mutations that exist in yeast occur in Sin3p, a protein that has been suggested to target the RPD3p histone deacetylase (83, 93, 94, 96, 97). Histone acetylation might therefore provide a mechanism complementary to the activity of the SWI/SNF complex in directing chromatin disruption.

ACKNOWLEDGMENTS

We are particularly grateful to Craig L. Peterson for communicating results before publication. We thank Kiyoe Ura for advice on the nucleosome mobility assays and Thuy Vo for manuscript preparation.

REFERENCES

1. **Almer, A., H. Rudolph, A. Hinnen, and W. Horz.** 1986. Removal of positioned nucleosomes from the yeast PHO5 promoter upon PHO5 induction releases additional activating DNA elements. EMBO J. **5:**2689–2696.
2. **Almer, A., and W. Horz.** 1986. Nuclease hypersensitive regions with adjacent positioned nucleosomes mark the gene boundaries of the PHO5/PHO3 locus in yeast. EMBO J. **5:**2681–2688.
3. **Arents, G., R. W. Burlingame, B. W. Wang, W. E. Love, and E. N. Moudrianakis.** 1991. The nucleosomal core histone octamer at 3.1Å resolution: a tripartite protein assembly and a left-handed superhelix. Proc. Natl. Acad. Sci. USA **88:**10148–10152.
4. **Arents, G., and E. N. Moudrianakis.** 1993. Topography of the histone octamer surface: repeating structural motifs utilized in the docking of nucleosomal DNA. Proc. Natl. Acad. Sci. USA **90:**10489–10493.
5. **Barlev, N. A., R. Candau, L. Wang, P. Darpino, N. Silverman, and S. L. Berger.** 1995. Characterization of physical interactions of the putative transcriptional adaptor ADA2 with acidic activation domains and TATA-binding-protein. J. Biol. Chem. **270:**19337–19343.
6. **Bashkin, J., J. J. Hayes, T. D. Tullius, and A. P. Wolffe.** 1993. Structure of DNA in a nucleosome core at high salt concentration and at high temperature. Biochemistry **32:**1895–1898.
7. **Baer, B. W., and D. Rhodes.** 1983. Eukaryotic RNA polymerase II binds to nucleosome cores from transcribed genes. Nature (London) **301:**482–488.
8. **Bauer, W. R., J. J. Hayes, J. H. White, and A. P. Wolffe.** 1994. Nucleosome structural changes due to acetylation. J. Mol. Biol. **236:**685–690.
9. **Beato, M., P. Herrlich, and G. Schultz.** 1995. Steroid hormone receptors: many actors in search of a plot. Cell **83:**851–857.
10. **Becker, P. B.** 1994. The establishment of active promoters in chromatin. Bioessays **16:**541–547.
11. **Birkenmeier, E. H., D. D. Brown, and E. Jordan.** 1978. A nuclear extract of *Xenopus laevis* oocytes that accurately transcribes 5S RNA genes. Cell **15:**1077–1086.
12. **Brownell, J. E., J. Zhou, T. Ranalli, R. Kobayashi, D. G. Edmondson, S. Y. Roth, and C. D. Allis.** 1996. Tetrahymena histone acetyltransferase A: a homolog to yeast Gcn5p linking histone acetylation to gene activation. Cell **84:**843–851.
13. **Burkhoff, A. M., and T. D. Tullius.** 1988. Structural details of an adenine tract that does not cause DNA to bend. Nature (London) **331:**455–457.
14. **Cairns, B. R., Y. J. Kim, M. H. Sayre, B. C. Laurent, and R. D. Kornberg.**

1994. A multisubunit complex containing the SWIA/ADR6, SWI2/SNF2, SWI3/SNF5 and SNF6 gene products isolated from yeast. Proc. Natl. Acad. Sci. USA **91:**1950–1954.
15. **Cairns, B. R., Y. Lorch, Y. Li, M. Zhang, L. Lacomis, H. Evdjument-Bromage, P. Tempst, J. Du, B. Laurent, and R. D. Kornberg.** 1996. RSC, an essential, abundant chromatin-remodeling complex. Cell **87:**1249–1260.
16. **Camerini-Otero, R. D., B. Sollner-Webb, and G. Felsenfeld.** 1976. The organization of histones and DNA in chromatin: evidence for an arginine-rich histone kernel. Cell **8:**333–347.
17. **Carlson, M., and B. C. Laurent.** 1994. The SNF/SWI family of global transcriptional activators. Curr. Opin. Cell Biol. **6:**396–402.
18. **Clark, D. J., and A. P. Wolffe.** 1991. Superhelical stress and nucleosome mediated repression of 5S RNA gene transcription *in vitro*. EMBO J. **10:**3419–3428.
19. **Clark-Adams, C. D., D. Norris, M. A. Osley, J. S. Fassler, and F. Winston.** 1988. Changes in histone gene dosage alter transcription in yeast. Genes Dev. **2:**150–159.
20. **Côté, J., J. Quinn, J. L. Workman, and C. L. Peterson.** 1994. Stimulation of GAL4 derivative binding to nucleosomal DNA by the yeast SWI/SNF complex. Science **265:**53–60.
21. **Dallas, P. B., P. Yaciuk, and E. Moran.** 1997. Characterization of monoclonal antibodies raised against p300: both p300 and CBP are present in intracellular TBP complexes. J. Virol. **71:**1726–1731.
22. **Dong, F., and K. E. van Holde.** 1991. Nucleosome positioning is determined by the $(H3\text{-}H4)_2$ tetramer. Proc. Natl. Acad. Sci. USA **88:**10596–10600.
23. **Dong, F., J. C. Hansen, and K. E. van Holde.** 1989. DNA and protein determinants of nucleosome positioning on sea urchin 5S rRNA gene sequences in vitro. Proc. Natl. Acad. Sci. USA **87:**5724–5728.
24. **Edmondson, D. G., M. M. Smith, and S. Y. Roth.** 1996. Repression domain of the yeast global repressor Tup1 interacts directly with histones H3 and H4. Genes Dev. **10:**1247–1259.
25. **Eickbusch, T. H., and E. N. Moudrianakis.** 1978. The histone core complex: an octamer assembled by two sets of protein-protein interactions. Biochemistry **17:**4955–4967.
26. **Fassler, J. S., and F. Winston.** 1988. Isolation and analysis of a novel class of suppressor of Ty insertion mutations in *Saccharomyces cerevisiae*. Genetics **118:**112–132.
27. **Fisher-Adams, G., and M. Grunstein.** 1995. Yeast histone H4 and H3 N-termini have different effects on the chromatin structure of the *Gal1* promoter. EMBO J. **14:**1468–1477.
28. **Freeman, L., H. Kurumizaka, and A. P. Wolffe.** 1996. Functional domains for assembly of histones H3 and H4 into the chromatin of *Xenopus* embryos. Proc. Natl. Acad. Sci. USA **93:**12780–12785.
29. **Gaudreau, L., A. Schmid, D. Blaschke, M. Ptashne, and W. Horz.** 1997. RNA polymerase II holoenzyme recruitment is sufficient to remodel chromatin at the yeast *PHO5* promoter. Cell **89:**55–62.
30. **Germond, J. E., B. Hirt, P. Oudet, M. Gross-Bellard, and P. Chambon.** 1975. Folding of the double helix in chromatin like structures from simian virus 40. Proc. Natl. Acad. Sci. USA **72:**1843–1847.
31. **Godde, J. S., and A. P. Wolffe.** 1995. Disruption of reconstituted nucleosomes: the effect of particle concentration $MgCl_2$, and KCl concentration, the histone tails and temperature. J. Biol. Chem. **270:**27399–27402.
32. **Godde, J. S., Y. Nakatani, and A. P. Wolffe.** 1995. The amino-terminal tails of the core histones and the translational position of the TATA box determine TBP/TFIIA association with nucleosomal DNA. Nucleic Acids Res. **23:**4557–4564.
33. **Grunstein, M., L. K. Durrin, R. K. Mann, G. Fisher-Adams, and L. M. Johnson.** 1992. Histones: regulators of transcription in yeast, p. 1295–1315. *In* S. McKnight and K. Yamamoto (ed.), Transcriptional regulation. Cold Spring Harbor Press, Cold Spring Harbor, N.Y.
34. **Han, M., and M. Grunstein.** 1988. Nucleosome loss activates yeast downstream promoters *in vivo*. Cell **55:**1137–1145.
35. **Han, M., U.-J. Kim, P. Kayne, and M. Grunstein.** 1988. Depletion of histone H4 and nucleosomes activates the PHO5 gene in *Saccharomyces cerevisiae*. EMBO J. **7:**2221–2228.
36. **Hansen, J. C., and A. P. Wolffe.** 1994. A role for histones H2A/H2B in chromatin folding and transcriptional repression. Proc. Natl. Acad. Sci. USA **91:**2339–2343.
37. **Hayes, J. J., and A. P. Wolffe.** 1992. Histone H2A/H2B inhibit the interaction of TFIIIA with 5S DNA in a nucleosome. Proc. Natl. Acad. Sci. USA **89:**1229–1233.
37a. **Hayes, J. J., and A. P. Wolffe.** 1993. Preferential and asymmetric interaction of linker histones with 5S DNA in the nucleosome. Proc. Natl. Acad. Sci. USA **90:**6415–6419.
38. **Hayes, J. J., T. D. Tullius, and A. P. Wolffe.** 1990. The structure of DNA in a nucleosome. Proc. Natl. Acad. Sci. USA **87:**7405–7409.
39. **Hayes, J. J., D. J. Clark, and A. P. Wolffe.** 1991. Histone contributions to the structure of DNA in the nucleosome. Proc. Natl. Acad. Sci. USA **88:**6829–6833.
40. **Hayes, J. J., J. Bashkin, T. D. Tullius, and A. P. Wolffe.** 1991. The histone core exerts a dominant constraint on the structure of DNA in a nucleosome. Biochemistry **30:**8434–8440.
41. **Herskowitz, I., B. Andrews, W. Kruger, J. Ogas, A. Sil, C. Coburn, and C. Peterson.** 1992. Integration of multiple regulatory inputs in the control of HO expression in yeast, p. 949–974. *In* S. McKnight and K. Yamamoto (ed.), vol. 2. Transcriptional regulation, vol. 2. Cold Spring Harbor Press, Cold Spring Harbor, N.Y.
42. **Hirschhorn, J. N., S. A. Brown, C. D. Clark, and F. Winston.** 1992. Evidence that SNF2/SWI2 and SNF activate transcription in yeast by altering chromatin structure. Genes Dev. **6:**2288–2298.
43. **Imbalzano, A. M., H. Kwon, M. R. Green, and R. E. Kingston.** 1994. Facilitated binding of TATA-binding protein to nucleosomal DNA. Nature **370:**481–485.
44. **Johnson, L. M., P. S. Kayne, E. S. Kahn, and M. Grunstein.** 1990. Genetic evidence for an interaction between SIR3 and histone H4 in the repression of silent mating loci in *Saccharomyces cerevisiae*. Proc. Natl. Acad. Sci. USA **87:**6286–6290.
45. **Karantza, V., E. Freire, and E. N. Moudrianakis.** 1996. Thermodynamic studies of the core histones: pH and ionic strength effects on the stability of the $(H3\text{-}H4)/(H3\text{-}H4)_2$ system. Biochemistry **35:**2037–2046.
46. **Kayne, P. S., U. J. Kim, M. Han, J. R. Mullen, F. Yoshizaki, and M. Grunstein.** 1988. Extremely conserved histone H4 N-terminus is dispensible for growth but essential for repressing the silent mating loci in yeast. Cell **55:**27–39.
47. **Khavari, P. A., C. L. Peterson, J. W. Tamkun, D. B. Mendel, and G. R. Crabtree.** 1993. BRG1 contains a conserved domain of the SWI2/SNF2 family necessary for normal mitotic growth and transcription. Nature **366:**170–174.
48. **Kruger, W., and I. Herskowitz.** 1991. A negative regulator of HO transcription, SIN1 (SPT2), is a nonspecific DNA binding protein related to HMG1. Mol. Cell. Biol. **11:**4135–4146.
49. **Kruger, W., C. L. Peterson, A. Sil, C. Coburn, G. Arents, E. N. Moudrianakis, and I. Herskowitz.** 1995. Amino acid substitutions in the structured domains of histones H3 and H4 partially relieve the requirement of the yeast SWI/SNF complex for transcription. Genes Dev. **9:**2770–2779.
50. **Kwon, H., A. N. Imbalzano, P. A. Khavarl, R. E. Kingston, and M. R. Green.** 1994. Nucleosome disruption and enhancement of activator binding by a human SWI/SNF complex. Nature **370:**477–481.
51. **Landsberger, N., and A. P. Wolffe.** 1995. The role of chromatin and *Xenopus* heat shock transcription factor (XHSF1) in the regulation of the *Xenopus hsp70* promoter in vivo. Mol. Cell. Biol. **15:**6013–6024.
52. **Landsberger, N., and A. P. Wolffe.** 1997. Remodeling of regulatory nucleoprotein complexes during meiotic maturation of the *Xenopus* oocyte. EMBO J. **16:**4361–4373.
53. **Laurent, B. C., and M. Carlson.** 1992. Yeast SNF2/SWI2, SNF5 and SNF6 proteins function coordinately with the gene-specific transcriptional activators Gal4 and bicoid. Genes Dev. **6:**1707–1715.
54. **Laurent, B. C., I. Treich, and M. Carlson.** 1993. The yeast SNF2/SWI2 protein has DNA stimulated ATPase activity required for transcriptional activation. Genes Dev. **7:**583–591.
55. **Lee, D. Y., J. J. Hayes, D. Pruss, and A. P. Wolffe.** 1993. A positive role for histone acetylation in transcription factor binding to nucleosomal DNA. Cell **72:**73–84.
56. **Lutter, L.** 1978. Kinetic analysis of deoxyribonuclease I cleavage sites in the nucleosome core: evidence for a DNA superhelix. J. Mol. Biol. **124:**391–420.
57. **Meersseman, G., S. Pennings, and E. M. Bradbury.** 1991. Chromatosome positioning on assembled long chromatin: linker histones affect nucleosome placement on 5S DNA. J. Mol. Biol. **220:**89–100.
58. **Meersseman, G., S. Pennings, and E. M. Bradbury.** 1992. Mobile nucleosomes-a general behavior. EMBO J. **11:**2951–2959.
59. **Mizzen, C. A., X. J. Yang, T. Kobuko, J. E. Brownell, A. J. Banister, T. Owen-Hughes, J. Workman, S. L. Berger, T. Kouzarides, Y. Nakatani, and C. D. Allis.** 1996. The $TAF_{II}250$ subunit of TFIID has histone acetyltransferase activity. Cell **87:**1261–1270.
60. **Muchardt, C., and M. Yaniv.** 1993. A human homolog of *Saccharomyces cerevisiae* SNF2/SWI2 and *Drosophila* brm genes potentiates transcriptional activation by the glucocorticoid receptor. EMBO J. **12:**4279–4290.
61. **Muchardt, C., C. Sardet, B. Bourachot, C. Onufryk, and M. Yaniv.** 1995. A human protein with homology to *S. cerevisiae* SNF5 interacts with the potential helicase hbrm. Nucleic Acids Res. **23:**1127–1132.
62. **Neigeborn, L., K. Rubin, and H. Carlson.** 1986. Suppressors of *snf2* mutations restore invertase derepression and cause temperature sensitive lethality in yeast. Genetics **112:**741–753.
63. **Noll, M., and R. D. Kornberg.** 1977. Action of micrococcal nuclease on chromatin and the location of histone H1. J. Mol. Biol. **109:**393–404.
64. **Ogryzko, V. V., R. L. Schiltz, V. Russanova, B. H. Howard, and Y. Nakatani.** 1996. The transcriptional coactivators p300 and CBP are histone acetyltransferases. Cell **87:**953–959.
65. **Perry, M., G. H. Thomson, and R. G. Roeder.** 1985. The nucleotide sequence and genomic organization of two distinct tandemly repeated *Xenopus laevis* histone gene clusters. J. Mol. Biol. **185:**479–499.
66. **Peterson, C. L., W. Kruger, and I. Herskowitz.** 1991. A functional interaction between the C-terminal domain of RNA polymerase II and the neg-

ative regulator SIN1. Cell **64:**1135–1143.
67. **Peterson, C. L., and I. Herskowitz.** 1992. Characterization of the yeast SWI1, SWI2 and SWI3 genes which encode a global activator of transcription. Cell **68:**573–584.
68. **Peterson, C. L., A. Dingwall, and M. P. Scott.** 1994. SWI/SNF gene products are components of a large multisubunit complex required for transcriptional enhancement. Proc. Natl. Acad. Sci. USA **91:**2905–2908.
69. **Peterson, C. L., and J. W. Tamkun.** 1995. The SWI/SNF complex: a chromatin remodeling machine? Trends Biochem. Sci. **20:**143–146.
70. **Peterson, C. L.** 1995. The SWI/SNF protein machine: helping transcription factors contend with chromatin-mediated repression. Nucleus **1:**185–206.
71. **Pruss, D., and A. P. Wolffe.** 1993. Histone-DNA contacts in a nucleosome core containing a *Xenopus* 5S rRNA gene. Biochemistry **32:**6810–6814.
72. **Pruss, D., J. J. Hayes, and A. P. Wolffe.** 1995. Nucleosomal anatomy—where are the histones? Bioessays **17:**161–170.
73. **Quinn, J., A. M. Fyrberg, R. W. Ganster, M. C. Schmidt, and C. L. Peterson.** 1996. DNA-binding properties of the yeast SWI/SNF complex. Nature **379:**844–847.
74. **Read, C. M., J. P. Baldwin, and C. Crane-Robinson.** 1985. Structure of subnucleosomal particles tetrameric $(H3/H4)_2$ 146 base pair and hexameric $(H3/H4)_2$ (H2A/H2B)1 146bp DNA complexes. Biochemistry **24:**4435–4450.
75. **Rhodes, D.** 1985. Structural analysis of a triple complex between the histone octamer, a Xenopus gene for 5S RNA and transcription factor IIIA. EMBO J. **4:**3473–3482.
76. **Roth, S. Y., A. Dean, and R. T. Simpson.** 1990. Yeast α2 repressor positions nucleosomes in TRP1/ARS1 chromatin. Mol. Cell. Biol. **10:**2247–2260.
77. **Roth, S. Y., M. Shimizu, L. Johnson, M. Grunstein, and R. T. Simpson.** 1992. Stable nucleosome positioning and complete repression by the yeast α2 repressor are disrupted by amino-terminal mutation in histone H4. Genes Dev. **6:**411–425.
78. **Simon, R. H., and G. Felsenfeld.** 1979. A new procedure for purifying histone pairs H2A+H2B and H3+H4 from chromatin using hydroxylapatite. Nucleic Acids Res. **6:**689–696.
79. **Simpson, R. T., and D. W. Stafford.** 1983. Structural features of a phased nucleosome core particle. Proc. Natl. Acad. Sci. USA **80:**51–55.
80. **Simpson, R. T., F. Thoma, and J. M. Brubaker.** 1985. Chromatin reconstituted from tandemly repeated cloned DNA fragments and core histones: a model system for study of higher order structure. Cell **42:**799–808.
81. **Svaren, J., and W. Horz.** 1995. Interplay between nucleosomes and transcription factors at the yeast PHO5 promoter. Semin. Cell Biol. **6:**177–183.
82. **Svaren, J., and W. Horz.** 1996. Regulation of gene expression by nucleosomes. Curr. Opin. Genet. Dev. **6:**164–170.
83. **Taunton, J., C. A. Hassig, and S. L. Schreiber.** 1996. A mammalian histone deacetylase related to a yeast transcriptional regulator Rpd3. Science **272:**408–411.
84. **Tsukiyama, T., P. B. Becker, and C. Wu.** 1994. ATP-dependent nucleosome disruption at a heat-shock promoter mediated by binding of GAGA transcription factor. Nature **367:**525–532.
85. **Tsukiyama, T., and C. Wu.** 1995. Purification and properties of an ATP dependent nucleosome remodeling factor. Cell **83:**1011–1020.
86. **Tullius, T. D., and B. A. Dombroski.** 1985. Iron (II) EDTA used to measure the helical twist along any DNA molecule. Science **230:**679–681.
87. **Ura, K., J. J. Hayes, and A. P. Wolffe.** 1995. A positive role for nucleosome mobility in the transcriptional activity of chromatin templates: restriction by linker histones. EMBO J. **14:**3752–3765.
88. **Ura, K., K. Nightingale, and A. P. Wolffe.** 1996. Differential association of HMG1 and linker histones B4 and H1 with dinucleosomal DNA: structural transitions and transcriptional repression. EMBO J. **15:**4959–4969.
89. **Ura, K., H. Kurumizaka, S. Dimitrov, G. Almouzni, and A. P. Wolffe.** 1997. Histone acetylation: influence on transcription by RNA polymerase, nucleosome mobility and positioning, and linker histone dependent transcriptional repression. EMBO J. **16:**2096–2107.
90. **Varga-Weisz, P. D., T. A. Blank, and P. B. Becker.** 1995. Energy-dependent chromatin accessibility and nucleosome mobility in a cell free system. EMBO J. **14:**2209–2216.
91. **Vettese-Dadey, M., P. A. Grant, T. R. Hebbes, C. Crane-Robinson, C. D. Allis, and J. L. Workman.** 1996. Acetylation of histone H4 plays a primary role in enhancing transcription factor binding to nucleosomal DNA *in vitro*. EMBO J. **15:**2508–2518.
92. **Vettesse-Dadey, M., P. Walter, H. Chen, L.-J. Juan, and J. L. Workman.** 1994. Role of the histone amino termini in facilitated binding of a transcription factor, GAL4-AH, to nucleosome cores. Mol. Cell. Biol. **14:**970–981.
93. **Vidal, M., R. Strich, R. E. Esposito, and R. F. Gaber.** 1991. RPD1 (SIN3/UME4) is required for maximal activation and repression of diverse yeast genes. Mol. Cell. Biol. **11:**6306–6316.
94. **Vidal, M., and R. F. Gaber.** 1991. RPD3 encodes a second factor required to achieve maximum positive and negative transcriptional states in *Saccharomyces cerevisiae*. Mol. Cell. Biol. **11:**6317–6327.
95. **Wall, G., P. D. Varga-Weisz, R. Sandaltzopoulos, and P. B. Becker.** 1995. Chromatin remodeling by GAGA factor and heat shock factor at the hypersensitive *Drosophila* hsp26 promoter *in vitro*. EMBO J. **14:**1727–1736.
96. **Wang, H., and D. J. Stillman.** 1993. Transcriptional repression in *Saccharomyces cerevisiae* by a SIN3-LexA fusion protein. Mol. Cell. Biol. **13:**1805–1814.
97. **Wang, H., I. Clark, P. R. Nicholon, I. Herskowitz, and D. J. Stillman.** 1990. The *Saccharomyces cerevisiae* SIN3 gene a negative regulator of HO contains four paired amphipathic helix motifs. Mol. Cell. Biol. **10:**5927–5936.
98. **Wechser, M. A., M. P. Kladde, J. A. Alfieri, and C. L. Peterson.** 1997. Effects of Sin versions of histone H4 on yeast chromatin structure and function. EMBO J. **16:**2086–2095.
99. **White, J. H., N. R. Cozzarelli, and W. R. Bauer.** 1988. Helical repeat and linking number of surface wrapped DNA. Science **241:**323–327.
100. **Wilson, C. J., D. M. Chao, A. N. Imbalzano, G. R. Schnitzer, R. Kingston, and R. A. Young.** 1996. RNA polymerase II holoenzyme contains SWI/SNF regulators involved in chromatin remodeling. Cell **84:**235–244.
101. **Winston, F., and M. Carlson.** 1992. Yeast SNF/SWI transcriptional activators and the SPT/SIN chromatin connection. Trends Genet. **8:**387–391.
102. **Wolffe, A. P.** 1994. Switched-on chromatin. Curr. Biol. **4:**525–527.
103. **Wolffe, A. P.** 1995. Chromatin: structure and function, 2nd ed. Academic Press, London, England.
104. **Wolffe, A. P., and J. J. Hayes.** 1993. The analysis of transcription factor interactions with model nucleosomal templates. Methods Mol. Genet. **2:**314–330.
105. **Wolffe, A. P., E. Jordan, and D. D. Brown.** 1986. A bacteriophage RNA polymerase transcribes through a *Xenopus* 5S RNA gene transcription complex without disrupting it. Cell **44:**381–389.
106. **Worcel, A., S. Han, and M. L. Wong.** 1978. Assembly of newly replicated chromatin. Cell **15:**969–977.
107. **Wray, W., T. Boulikas, V. Wray, and R. Hancock.** 1981. Silver staining of proteins in polyacrylamide gels. Anal. Biochem. **118:**197–203.
108. **Yang, X.-J., V. V. Ogryzko, J.-I. Nishikawa, B. Howard, and -Y. Nakatani.** 1996. A p300/CBP-associated factor that competes with the adenoviral E1A oncoprotein. Nature **382:**319–324.
109. **Yoshinaga, S. K., S. L. Peterson, I. Herskowitz, and K. R. Yamamoto.** 1992. Roles of SWI1, SWI2, and SWI3 proteins for transcriptional enhancement by steroid receptors. Science **258:**1598–1604.